Supporting Information

Reaction Site-Driven Regioselective Synthesis of AChE Inhibitors

Emilia Oueis, Gianluca Santoni, Cyril Ronco, Olga Syzgantseva, Vincent Tognetti, Laurent Joubert, Anthony Romieu, Martin Weik, Ludovic Jean, Cyrille Sabot*, Florian Nachon and Pierre-Yves Renard**

CAUTION! All of the compounds described here (and especially the most potent bivalent inhibitors) are potentially neurotoxic. They must be handled with extreme care by trained personnel.

List of contents

I. General information and materials

All solvents were dried following standard procedures; CH_3CN: distillation over P_2O_5; Triethylamine (TEA) distillation over CaH_2. Anhydrous DMF stocked over 4 Å molecular sieves was purchased from Carlo Erba. The HPLC-gradient grade acetonitrile (CH_3CN) and methanol (MeOH) were purchased from VWR. Aq. buffers (currently used for IC_{50} determinations and *in situ* click chemistry experiments) and mobile-phases for HPLC were prepared using water purified with a Milli-Q system (purified to 18.2 MΩ.cm). ^1H and ^{13}C NMR spectra (C13APT or C13CPD experiments) were recorded on a Bruker DPX 300 spectrometer. Chemical shifts are expressed in parts per million (ppm) from CD_3OD (δH = 3.31, δC = 49.00).[1] ^1J values are expressed in Hz. Low-resolution mass spectra were obtained with a Finnigan LCQ Advantage MAX (ion trap) apparatus equipped with an electrospray ionization source. High-resolution mass spectra (HRMS) were obtained with a Waters LCT Premier XE mass spectrometer. IR spectra were recorded with a universal attenuated total reflectance (ATR) sampling accessory on a Perkin-Elmer FTIR Spectrum 100 spectrometer. Several chromatographic systems were used for the purification steps and the analytical experiments. System A: semi-preparative HPLC purification steps on a reversed-phase HPLC column (C_{18}, Thermo Hypersil GOLD, 5 µm, 21.2 × 250 mm) with CH_3CN and trifluoroacetic acid 0.1% (TFA 0.1%, pH 2.0) as eluents [100% TFA (5 min), then linear gradient from 0% to 100% of CH_3CN (60 min)] at a flow rate of 16.0 mL/min with dual UV detection achieved at 240 and 350 nm. System B: System A with the following gradient [100% TFA (5 min), then linear gradient from 0% to 20% of CH_3CN (20 min), then a linear gradient to 40% of CH_3CN (15 min), then an isocratic mode at 40% of CH_3CN (5 min), then a linear gradient to 60% of CH_3CN (15 min), then an isocratic mode at 60% of CH_3CN (5 min) and finally a linear gradient to 100% of CH_3CN (20 min)]. System C: analytical RP-HPLC was performed on a Thermo Scientific Surveyor Plus instrument equipped with a PDA detector and a Thermo Hypersil GOLD C_{18} column (5 µm, 4.6 × 100 mm) with CH_3CN and 0.1% aqueous TFA system [100% TFA (5 min), linear gradient from 0% to 67% of CH_3CN (20 min), then 67% to 100% of CH_3CN (25min)] at a flow rate of 1.0 mL/min. UV-vis detection with the "Max Plot" mode, chromatogram at maximum absorbance of each compound (220-360 nm), was used to determine the compounds purity. System D: LCMS/SIM experiments were performed on a Thermo Scientific Surveyor Plus instrument; reversed-phase HPLC separation was achieved with a 5 µm, 2.1 × 150 mm Thermo Hypersil

GOLD C_{18} column equipped with a C_{18} guard column. The solvent system consisted of a linear gradient of CH_3CN in aqueous formic acid 0.1% (FA 0.1%, pH 2.7) at a flow rate of 0.25 mL/min. ESI detection in the positive mode (Full scan, 150-2000 a.m.u., SIM mode, 3 ranges each centered on the expected molecular weight of compound, mono-oxidized compound and dioxidized compound (Fig. 1) and their doubly charged ions; data type: centroid, sheat gas fow: 60 arb unit, aux/sweep gas flow rate: 20 arb unit, spray voltage: 4.5 kV, capillary temp: 270 °C, capillary voltage: -10 V, tube lens offset: -50 V).

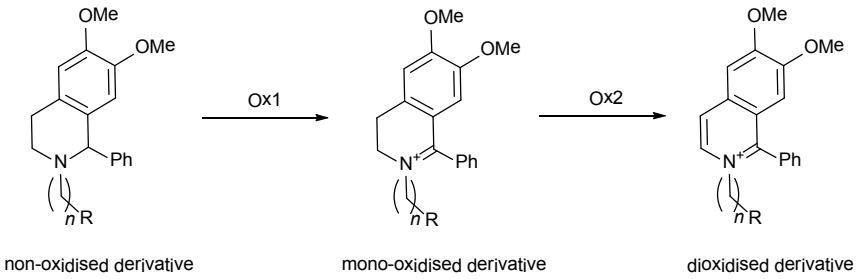

Figure 1: Oxidation of PIQ derivatives affording the mono- and dioxidized products.

II. Experimental procedures

Huprine and PIQ precursors for the *in situ* click chemistry experiments (*i.e.*, azide and alkyne derivatives, respectively) were synthesized according to the procedures previously described by our group [2] and Sharpless *et al.*[3]

II.1 Synthetic procedures

***Anti*-9-HUPZ4PIQ-A1**

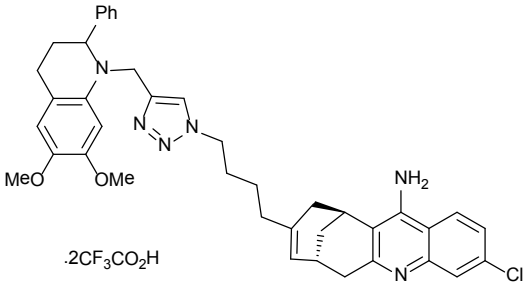

A mixture of azide **9-HUPZ4** (6.2 mg, 16.3 µmol), alkyne **PIQ-A$_1$** (5.1 mg, 16.3 µmol) and copper iodide (2.5 mg, 13.0 µmol) in dry CH_3CN (0.5 mL) was stirred at r.t., under Ar atmosphere, with light protection for 10 days. The reaction mixture was concentrated to dryness then purified by semi-preparative RP-HPLC (system A) to afford after freeze-drying the corresponding heterodimer ***Anti*-9-HUPZ4PIQ-A1** as white amorphous solid (10.9 mg,

74%). ^{1}H (300 MHz, CD_3OD) δ = 1.25-1.33 (m, 2H), 1.59-1.75 (m, 2H), 1.93-2.10 (m, 5H), 2.5 (dd, *J* = 17.7 Hz, *J* = 3.9 Hz, 1H), 2.80-2.81 (m, 1H), 2.9 (d, *J* = 19.8 Hz, 1H), 3.20 (d, *J* = 5.7 Hz, 1H), 3.25-3.35 (m, 3H), 3.39-3.43 (m, 2H), 3.50-3.56 (m, 1H), 3.61 (s, 3H), 3.65-3.72 (m, 1H), 3.87 (s, 3H), 4.27-4.36 (m, 2H), 5.61 (d, *J* = 4.5 Hz, 1H), 5.85 (s, 1H), 6.36 (s, 1H), 6.92 (s, 1H), 7.38-7.40 (m, 2H), 7.50-7.52 (m, 3H), 7.57 (dd, *J* = 9.1 Hz, *J* = 1.7 Hz, 1H), 7.73 (d, *J* = 1.7 Hz, 1H), 8.07 (s, 1H), 8.34 (d, *J* = 9.1 Hz, 1H); ^{13}C (75 MHz, CD_3OD) δ = 25.1, 27.5, 28.1, 29.3, 30.4, 33.8, 35.9, 37.2, 48.5, 51.2, 52.3, 56.4, 56.5, 67.2, 112.3 (2C), 115.3, 115.4, 119.3, 123.3, 124.8, 125.5, 126.3, 127.7, 127.8, 130.5 (3C), 131.4 (2C), 132.1, 137.7, 134.0, 139.5, 140.4, 150.1, 151.2 (2C), 153.0, 156.7; IR (neat) cm^{-1}: 3361, 3220, 2944, 1662, 1590, 1514, 1467, 1414, 1179, 1122, 834, 793, 720, 704; LR-MS (ESI+) *m/z* (%): 677.33 (65), 675.40 (100) $[M+H]^+$, 338.27 (85) $[M + 2H]^{2+}$; HRMS (ESI+): Calc. for $C_{40}H_{43}ClN_6O_2[M+H]^+$: 675.3209; found: 675.3227; RP-HPLC (system C) t_R =16.4 min (purity >95%); IC_{50} *m*-AChE = 0.63 ± 0.1 nM; IC_{50} *rh-AChE* = 3.31 ± 0.20 nM.

Anti-9-HUPZ4PIQ-A2

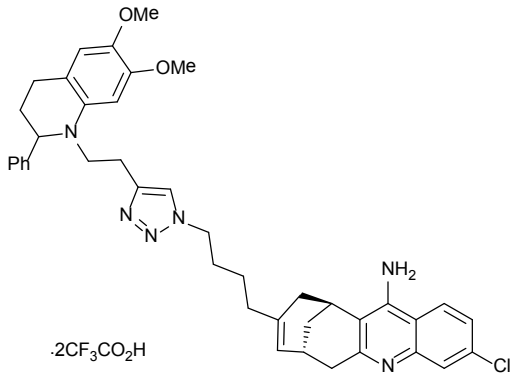

A mixture of azide **9-HUPZ4** (19.0 mg, 51.6 µmol), alkyne **PIQ-A$_2$** (20.1 mg, 62.5 µmol) and copper iodide (2.0 mg, 10.5 µmol) in dry CH_3CN (1 mL) was stirred at r.t., under Ar atmosphere, with light protection for 24 h. The reaction mixture was concentrated to dryness then purified by semi-preparative RP-HPLC (system A) to afford after freeze-drying the corresponding heterodimer ***Anti*-9-HUPZ4PIQ-A2** as light yellow amorphous solid (31.1 mg, 66%). ^{1}H (300 MHz, CD_3OD) δ = 1.25-1.37 (m, 2H), 1.59-1.73 (m, 2H), 1.90-2.20 (m, 5H), 2.48 (dd, *J* = 17.7 Hz, *J* = 3.9 Hz, 1H), 2.80 (s, 1H), 2.87 (d, *J* = 18.3 Hz, 1H), 3.21 (dd, *J* = 17.7 Hz, *J* = 5.5 Hz, 1H), 3.23-3.36 (m, 6H), 3.35-3.40 (m, 1H), 3.50-3.55 (m, 2H), 3.62 (s, 3H), 3.87 (s, 3H), 4.21 (t, *J* = 6.8 Hz, 2H), 5.58 (d, *J* = 4.7 Hz, 1H), 5.87 (s, 1H), 6.39 (s, 1H), 6.93 (s, 1H), 7.35-7.39 (m, 2H), 7.46-7.51 (m, 3H), 7.56 (dd, *J* = 9.0 Hz, *J* = 1.9 Hz, 1H), 7.73 (d, *J* = 1.7 Hz, 1H), 7.78 (s, 1H), 8.34 (d, *J* = 9.0 Hz, 1H); ^{13}C (75 MHz, CD_3OD) δ = 21.6, 24.2, 25.0, 27.5, 28.1, 29.3, 30.4, 33.9, 35.9, 37.2, 45.9, 51.0, 53.5, 56.4, 56.5, 67.5, 112.3

(2C), 115.3, 115.4, 119.2, 122.9, 124.2, 124.7, 125.4, 126.3, 127.7, 130.4 (3C), 131.4 (2C), 131.9, 138.0, 139.5, 140.4, 150.1, 151.2 (2C), 153.0, 156.7; LR-MS (ESI+) *m/z* (%): 689.27 (100), 345.13 (37) $[M + 2H]^{2+}$; IR (neat) cm^{-1}: 3355, 3208, 2933, 1664, 1591, 1514, 1461, 1414, 1176, 1120, 834, 799, 719, 704; HRMS (ESI+): Calc. for $C_{41}H_{45}ClN_6O_2[M + H]^+$: 689.3365; found: 689.3354; RP-HPLC (system C) t_R =16.3 min (purity >95%); IC_{50} *m*-AChE =0.40 ± 0.1 nM; IC_{50} *rh-AChE* = 0.64 ± 0.04 nM.

Anti-9-HUPZ4PIQ-A3

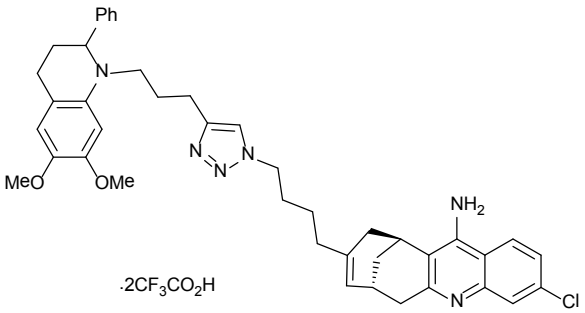

A mixture of azide **9-HUPZ4** (19.0 mg, 51.6 µmol), alkyne **PIQ-A$_3$** (20.1 mg, 60 µmol) and copper iodide (2.0 mg, 10.5 µmol) in dry CH_3CN (1 mL) was stirred at r.t. with light protection for 24 h. The reaction mixture was concentrated to dryness then purified by semi-preparative RP-HPLC (system A) to afford after freeze-drying the corresponding heterodimer ***Anti*-9-HUPZ4PIQ-A3** as a white amorphous solid (35.3 mg, 74%).^{1}H (300 MHz, CD_3OD) δ = 1.29-1.36 (m, 2H), 1.58-1.74 (m, 2H), 1.91-1.98 (m, 3H), 2.00-2.13 (m, 2H), 2.12-2.29 (m, 2H), 2.49 (dd, *J* = 18.0 Hz, *J* = 4.1 Hz, 1H), 2.69-2.78 (m, 2H), 2.78-2.83 (m, 1H), 2.87 (d, *J* = 18.1 Hz, 1H), 3.21 (dd, *J* = 17.6 Hz, *J* = 5.2 Hz, 1H), 3.18-3.35 (m, 4H), 3.33-3.56 (m, 3H), 3.59 (s, 3H), 3.86 (s, 3H), 4.20 (t, *J* = 7.1 Hz, 2H), 5.59 (d, *J* = 4.9 Hz, 1H), 5.74 (s, 1H), 6.32 (s, 1H), 6.90 (s, 1H), 7.29-7.33 (m, 2H), 7.44-7.47 (m, 3H), 7.57 (dd, *J* = 9.1 Hz, *J* = 1.9 Hz, 1H), 7.64 (s, 1H), 7.73 (d, *J* = 1.9 Hz, 1H), 8.35 (d, *J* = 9.1 Hz, 1H); ^{13}C (75 MHz, CD_3OD) δ = 23.3, 24.2, 24.7, 25.1, 27.5, 28.1, 29.3, 30.4, 33.9, 35.9, 37.2, 46.7, 51.0, 53.9, 56.3, 56.4, 67.9, 112.3, 112.5, 115.3, 115.4, 119.2, 123.2, 124.7, 124.8, 125.4, 126.3, 127.7, 130.4 (3C), 131.3 (2C), 131.6, 138.0, 139.5, 140.4, 150.0, 151.1 (2C), 153.0, 156.7; IR (neat) cm^{-1}: 3378, 3220, 2936, 1665, 1590, 1518, 1466, 1414, 1199, 1122, 829, 799, 719, 704; LR-MS (ESI+) *m/z* (%): 703.27 (28), 352.40 (100) $[M + 2H]^{2+}$; HRMS (ESI+): Calc. for $C_{42}H_{47}ClN_6O_2$ $[M + H]^+$: 703.3522; found: 703.3538; RP-HPLC (system C) t_R =16.3 min (purity >95%); IC_{50} *m*-AChE = 0.60 ± 0.2 nM; IC_{50} *rh-AChE* = 0.61 ± 0.1 nM.

Anti-9-HUPZ4PIQ-A4

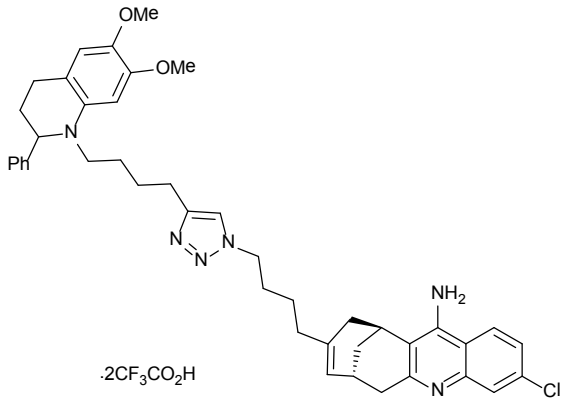

A mixture of azide **9-HUPZ4** (30.6 mg, 58.0 µmol), alkyne **PIQ-A$_4$** (24.8 mg, 72 µmol) and copper iodide (3.6 mg, 19 µmol) in dry CH_3CN (1.2 mL) and MeOH (0.3 mL) was stirred at r.t., under Ar atmosphere, with light protection for 16 h. The reaction mixture was concentrated to dryness then purified by semi-preparative RP-HPLC (system B) to afford after freeze-drying the corresponding heterodimer ***Anti*-9-HUPZ4PIQ-A4** as white amorphous solid (21.5 mg, 32%).^{1}H (300 MHz, CD_3OD) δ = 1.28-1.37 (m, 4H), 1.54-1.70 (m, 4H), 1.84-1.99 (m,5H), 2.00-2.15 (m, 2H), 2.48 (dd, *J* = 17.5 Hz, *J* = 3.9 Hz, 1H), 2.65-2.75 (m, 2H), 2.78-2.82 (m, 1H), 2.87 (d, *J* = 17.7 Hz, 1H), 3.21 (dd, *J* = 17.7 Hz, *J* = 5.5 Hz, 1H), 3.18-3.31 (m, 2H), 3.35-3.48 (m, 3H), 3.60 (s, 3H), 3.86 (s, 3H), 4.20 (t, *J* = 6.8 Hz, 2H), 5.59 (d, *J* = 5.1 Hz, 1H), 5.74 (s, 1H), 6.33 (s, 1H), 6.91 (s, 1H), 7.32-7.36 (m, 2H), 7.47-7.50 (m, 3H), 7.57 (dd, *J* = 9.0 Hz, *J* = 1.9 Hz, 1H), 7.71 (s, 1H), 7.72 (d, *J* = 1.9 Hz, 1H), 8.34 (d, *J* = 9.0 Hz, 1H); ^{13}C (75 MHz, CD_3OD) δ = 24.7, 25.1, 25.5, 27.3, 27.5, 28.1, 29.3, 30.4, 32.7, 33.8, 35.9, 37.2, 49.1, 51.0, 54.0, 56.4, 56.5, 67.8, 112.3 (2C), 115.3, 115.4, 119.2, 123.3, 124.8, 124.9, 125.5, 126.3, 127.7, 130.4 (3C), 131.3 (2C), 131.6, 138.0, 139.5, 140.4, 150.0, 151.1 (2C), 153.0, 156.7; IR (neat) cm^{-1}: 3367, 3220, 2939, 1662, 1584, 1514, 1467, 1414, 1176, 1120, 828, 800, 719, 703; LR-MS (ESI+) *m/z* (%): 717.40 (28), 359.33 (100) $[M + 2H]^{2+}$; HRMS (ESI+): Calc. for $C_{43}H_{49}ClN_6O_2$ $[M + H]^+$: 717.3678; found: 717.3690; RP-HPLC (system C) t_R =16.6 min (purity >95%); IC_{50} *m*-AChE = 1.20 ± 0.2 nM; IC_{50} *rh-AChE* = 0.78 ± 0.10 nM.

Anti-9-HUPZ2PIQ-A4

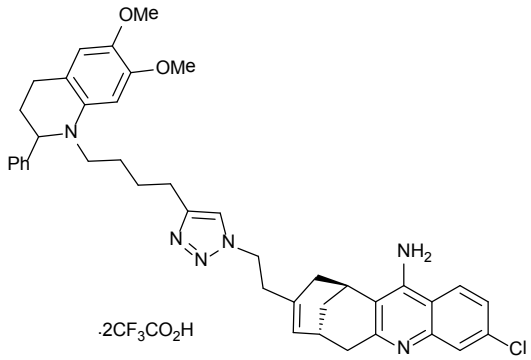

A mixture of azide **9-HUPZ2** (19 mg, 56 μmol), alkyne **PIQ-A$_4$** (20 mg, 57 μmol), copper iodide (11 mg, 56 μmol) and anhydrous TEA (10 μL, 70 μmol) in dry DMF (1 mL) was stirred at r.t. with light protection for 5 days under an Ar atmosphere. Thereafter, the crude mixture was partitioned between CH_2Cl_2 and deionized water (5 mL of each) and the aqueous phase was extracted with CH_2Cl_2 (2 × 5 mL). The combined organic layers were washed with deionized water (5 mL) and brine (5 mL), dried over anhydrous Na_2SO_4 and concentrated under reduced pressure to afford a brown yellowish solid. Purification by semi-preparative RP-HPLC (system B) afforded after freeze-drying the corresponding heterodimer ***Anti*-9-HUPZ2PIQ-A4** as light yellow amorphous solid (7.0 mg, 14%).^{1}H (300 MHz, CD_3OD) δ = 1.53-1.63 (m, 2H), 1.75-1.93 (m, 3H), 1.99-2.01 (m, 2H), 2.41-2.61 (m, 5H), 2.65-2.71 (m, 2H), 3.10-3.23 (m, 5H), 3.38-3.53 (m, 3H), 3.60 (s, 3H), 3.86 (s, 3H), 4.32 (t, *J* = 6.7 Hz, 2H), 5.48 (d, *J* = 5.0 Hz, 1H), 5.72 (s, 1H), 6.33 (s, 1H), 6.91 (s, 1H), 7.31-7.35 (m, 2H), 7.48-7.50 (m, 3H), 7.51 (s, 1H), 7.6 (dd, *J* = 9.1 Hz, *J*= 2.1 Hz, 1H), 7.8 (d, *J* = 1.8 Hz, 1H), 8.344 (d, *J* = 9.1 Hz, 1H); ^{13}C (75 MHz, CD_3OD) δ = 24.7,25.5, 27.3 (2C), 27.4, 28.0, 28.9, 33.4, 35.5, 35.8, 38.2, 51.1, 54.3, 56.4, 56.5, 67.8, 112.4 (2C), 115.1, 115.5, 119.3, 122.9, 124.8, 124.9, 126.4, 127.6, 128.3, 130.4 (3C), 131.4 (2C), 131.6, 134.4, 139.1, 139.7, 140.4, 150.1, 151.1, 152.7, 156.8; IR (neat) cm^{-1}: 3355, 3103, 2938, 1662, 1596, 1514, 1461, 1414, 1197, 1174, 1119, 828, 800, 718, 699; LR-MS (ESI+) *m/z* (%): 689.27 (18), 345.27 (100) $[M + 2H]^{2+}$; HRMS (ESI+): Calc. for $C_{41}H_{45}ClN_6O_2$ $[M + H]^+$: 689.3365; found: 689.3381; RP-HPLC (system C) t_R =15.8 min (purity >95%); IC_{50} *m*-AChE = 13.0 ± 2.5 nM; IC_{50} *rh-AChE* = 5.35 ± 0.3 nM.

***Anti*-12-HUPZ2PIQ-A6**

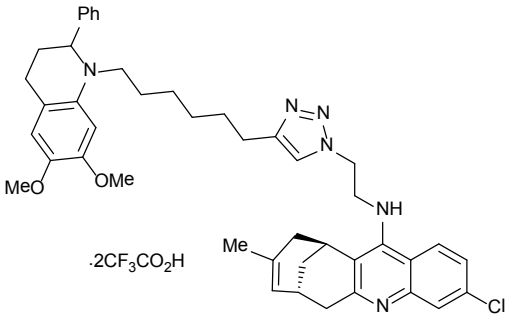

A mixture of azide **12-HUPZ2** (19 mg, 54 µmol), alkyne **PIQ-A$_6$** (27 mg, 70 µmol), copper(II) sulfate pentahydrate (3.0 mg, 10 µmol) and sodium ascorbate (4.5 mg, 20 µmol) in H_2O/EtOH/CH_2Cl_2 (1 : 1 : 1, v/v/v, 0.9 mL) was stirred at r.t. for 5 days under an Ar atmosphere. A same further amount of the catalyst system was added after 3 days. Thereafter, the reaction mixture was filtered on cotton and the filtrate evaporated to dryness then purified by semi-preparative RP-HPLC (system B) to afford after freeze-drying the corresponding heterodimer ***Anti*-12-HUPZ2PIQ-A6** as light yellow amorphous solid (10 mg, 19%).^{1}H (300 MHz, CD_3OD) δ = 1.30-1.38 (m, 4H), 1.55-1.59 (m, 5H), 1.73-1.89 (m, 3H), 2.0 (dd, *J* = 42.6 Hz, *J* = 12.5 Hz, 2H), 2.48 (br, s, 1H),2.57 (t, *J* = 7.5 Hz, 2H), 2.77 (br, s, 1H), 2.9 (d, *J* = 17.9 Hz, 1H),3.20 (dd, *J* = 5.2 Hz, *J* = 18.0 Hz, 1H),3.12-3.26 (m, 4H), 3.37-3.54 (m, 3H), 3.60 (s, 3H), 3.87 (s, 3H), 4.52-4.54 (m, 2H), 4.78-4.80 (m, 2H), 5.6 (d, *J* = 3.3 Hz, 1H), 5.74 (s, 1H), 6.35 (br, s, 1H), 6.92 (s, 1H), 7.34-7.37 (m, 2H), 7.48-7.51 (m, 3H), 7.56 (dd, *J* = 2.1 Hz, *J* = 9.3 Hz, 1H),7.71 (s, 1H), 7.76 (d, *J* = 2.1 Hz, 1H), 8.3 (d, *J* = 9.3 Hz, 1H); ^{13}C (75 MHz, CD_3OD) δ = 23.4, 24.1, 25.1, 26.0, 26.6, 27.3, 27.4, 27.8, 29.2, 29.6, 30.2, 36.0 (2C), 49.3, 51.0, 54.5, 56.4, 56.5, 67.8, 112.3 (2C), 115.9, 119.1, 119.3, 123.8, 124.8, 125.1, 127.1, 129.0, 130.4 (3C), 131.4 (2C), 131.7, 134.7, 137.1, 140.3, 140.7, 149.4, 150.1, 151.2 (C), 152.2, 157.5; IR (neat) cm^{-1}: 3302, 3073, 2944, 1669, 1578, 1520, 1461, 1414, 1197, 1174, 1120, 834, 799, 717, 699; LR-MS (ESI+) *m/z* (%): 731.27 (15), 366.33 (100) $[M + 2H]^{2+}$; HRMS (ESI+): Calc. for $C_{44}H_{51}ClN_6O_2$ $[M + H]^+$: 731.3835; found: 731.3829; RP-HPLC (system C) t_R =17.3 min (purity >95%); IC_{50} *m*-AChE = 7.01 ± 1.0 nM; IC_{50} *rh-AChE* = 6.1 ± 0.8 nM.

II.2. Experimental details

II.2.1. AChE inhibition assay

The inhibitory activity was evaluated spectrophotometrically using a UV-vis Varian Cary 50 scan spectrophotometer equipped with a microplate reader at 25 °C by the method of Ellman

using recombinant human AChE or mouse AChE[2b, 4] and acetylthiocholine iodide (0.50 mM) as substrate.[5] The reaction was performed in the presence of 40 pM of AChE in a final volume of 200 µL of 0.1 M phosphate-buffered solution (pH 7.4) containing 0.025% (25 mg per 100 mL) of bovine serum albumin (BSA) and 300 µM 5,5'- dithiobis-2-nitrobenzoic acid (DTNB) solution used to produce the yellow anion of 5-thio-2-nitrobenzoic acid. The different derivatives were pre-incubated with the enzyme at 25 °C for 90 min before UV absorbance measurement. One sample without inhibitor was always present to yield 100% of cholinesterase activity. One blank sample containing only DTNB was always present to yield the minimum absorbance of non-specific hydrolysis. The rate of change of absorbance ($\Delta Abs\text{min}^{-1}$), which reflects the rate of hydrolysis of acetylthiocholine, was recorded at 414 nm for 20 min (kinetics mode). These experiments were done in triplicate, the values were averaged and minimum absorbance subtracted. Data from concentration-response experiments of the inhibitors were analyzed by nonlinear regression using ProFit (Quantum Soft, Switzerland), which gave estimates of the IC_{50} values (concentration of drug producing 50% of enzyme activity inhibition). Recombinant human acetylcholinesterase was purified as previously described.[6] DTNB and acetylthiocholine iodide were purchased from Sigma.

II.2.2. In situ click reaction experiments

- **Preparation of ligands solutions**

10 mM methanolic solutions of acylation site ligand and peripheral site ligand were first prepared. These stock solutions were diluted with ammonium citrate buffer (2.0 mM ammonium citrate, 100 mM NaCl, pH 7.4) to afford 100 µM aqueous solutions (containing 1% of MeOH) of each ligand.

- **Enzymatic inhibitor assembly**

To ~1µM solutions of AChE (*rh or m*) in 2.0 mM ammonium citrate buffer (100 mM NaCl, pH 7.3-7.5), the previously prepared acylation site ligands huprine components (**9-HUPZ4, 9-HUPZ2 and 12-HUPZ2**) in ammonium citrate buffer were added followed by the corresponding peripheral site ligand coupling partner (**$PIQA_n$**) (5 eq.). The resulting solutions were thoroughly mixed, completed by the addition of MeOH (12 µL). The final concentrations were: AChE, 1 µM; huprine component, 4.6 µM, $PIQA_n$ component, 24 µM; MeOH, 1.5% with a total volume of 1 mL. Each reaction mixture was allowed to stand in a

laboratory oven at 37 °C. The enzyme was found to be stable in these experimental conditions as can be seen from the chart in figure 2.

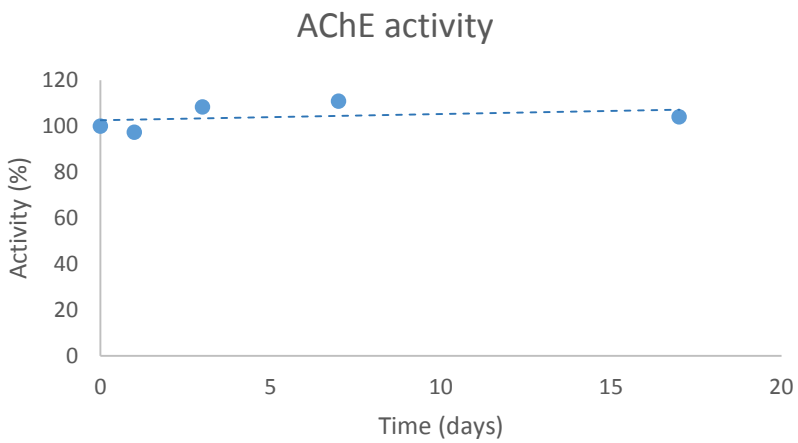

Figure 2: Chart representing the activity over time of *m*-AChE in the *in situ* click chemistry experimental conditions.

At regular intervals, aliquots of 50 µL were sampled and added to 50 µL of MeOH (for denaturation of the enzyme), and then the mixture was vortexed for 3 min, placed in an ultra sound bath for 5 min and lastly centrifuged. Finally, 20 µL of the solution were analyzed by LC/MS-SIM following system D. Parallel control experiments relative to the AChE-directed cycloaddition of HUP and PIQAn were conducted in the absence of AChE (buffer alone with ligand partners) and failed to give adduct detectable by LC-MS. Parallel control experiments relative to the AChE-directed cycloaddition of HUP and PIQAn were conducted in the absence of AChE (buffer alone with ligand partners) and failed to give adduct detectable by LC-MS (Figure 3).

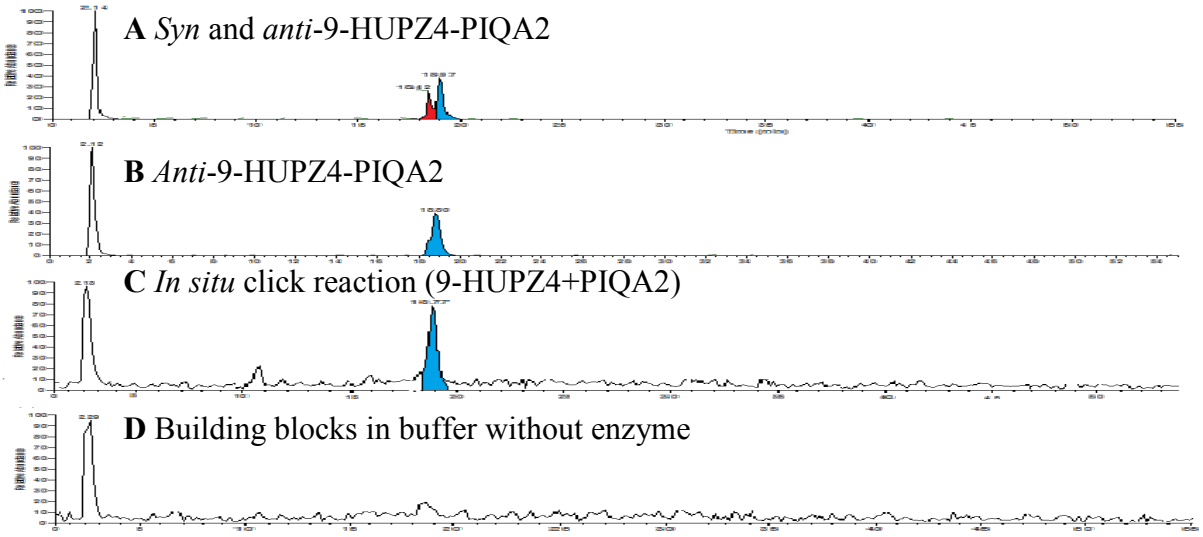

Figure 3: LCMS/SIM traces comparison of authentic samples of *syn* and *anti* **9-HUPZ4-PIQA2** (A and B) and traces of the click and blank experiments (C and D, respectively), showing the regioselective *in situ* formation of ***anti*-9-HUPZ4-PIQA2.**

III. Theoretical chemistry

III.1. Molecular dynamics-assisted docking

Since no experimental structure is available for the regioisomers of **9-HUPZ4PIQ-A2** in complex with human AChE, molecular dynamics-assisted docking was performed in order to get the best model possible of these complexes. Molecular dynamics improve docking performance by allowing backbone breathing, and thus better relaxation of the complex.

The structure of human AChE was prepared from the crystal structure of human AChE in complex with huprine W and fasciculin 2.[7] Missing *N*-terminal residues were rebuilt and minimized with MODELLER 9v8.[8] Crystallographic water molecules were conserved in the model. In order to sample the heterogeneity of the peripheral site residue Trp286 that is observed upon ligand binding, we prepared two different human AChE models reproducing the conformations of Trp286 of pdb structures 1Q83 (sandwiched) and 1Q84 (native). These structures represent alternative peripheral site conformations of mouse AChE in complex with **TZ2PIQ-A6**, a ligand structurally similar to **9-HUPZ4PIQ-A2**. The molecular models of each double protonated regioisomer of **9-HUPZ4PIQ-A2** and their four diastereoisomers were built and minimized with phenix elbow.[9] Each diastereoisomer was manually docked to both human AChE models by superimposing the huprine substructure to that observed in the human AChE/huprine W complex, then superimposing the PIQ substructure to the phenanthridinium substructure observed in the TZ2PA6/mouse AChE complex. Then, each resulting complex was simulated as follows. Molecular dynamics simulations were carried out using GROMACS 4.5.6[10] and the Amber99sb force field.[11] The topological description of each regio- and diastereoisomers of **9-HUPZ4PIQ-A2** was built using acpype and the general amber force field.[12] The complex was immersed in a periodic water box of cubic shape with a minimal distance of 10 Å to any edge and periodic boundary conditions. The box was solvated using the TIP3P solvation model and chloride and sodium counter ions at a concentration of 20 mM were added to neutralize the simulation system. After energy minimization using a 500-step steepest decent method, the system was subjected to equilibration at 310 K and 1 bar for 50 ps under the conditions of position restraints for heavy

atoms. The Lennard-Jones interactions were cut off at 1.4 nm. The long-range electrostatic interactions were handled using particle-mesh Ewald method for determining long-range electrostatics (9 Å cutoff). Temperature was set to 310 K and was kept constant using a Berendsen thermostat[13] (with a coupling time constant of 0.1 ps). Pressure with a reference value of 1 bar was controlled by a Berendsen barostat (with a coupling time constant of 0.5 ps). Full MD simulation was performed for 1 ns at 310 K, using 2 femtosecond timesteps. All bond lengths were constrained using the LINCS algorithm.[14] Coordinates were saved every 500 steps (every ps). The resulting conformation was optimized by a final 500-step steepest descent minimization.

Estimated total Gibbs free energy of binding in kcal/mol was calculated for the energy-minimized complex after the position restraints molecular dynamics and after the full molecular dynamics, using the scoring function of AutodockVina (version 1.1.1 ; option --score_only).[15] The receptor/ligand system was prepared with Autodock Tools 1.5.4.[16] without removing water molecules. The 3D affinity grid box was designed to include the full active site gorge of human AChE. For each regioisomer, each diastereoisomer and each enzyme conformation, the complex displaying the lowest energy of binding after the full molecular dynamics (≈ -16 kcal/mol) was selected for simulating the click-reaction by QM/MM (table 1). The lowest energy complex was achieved when using the conformation of Trp286 observed in the crystal structure of pdb code 1Q84 and in the crystal structure of the human AChE in the apostate (pdb code 3LII and 4EY4).

Table 1: Energies of all four diastereoisomers of each regioisomer in both enzyme conformations after the position restraints MD and the full 1 ns MD simulations.

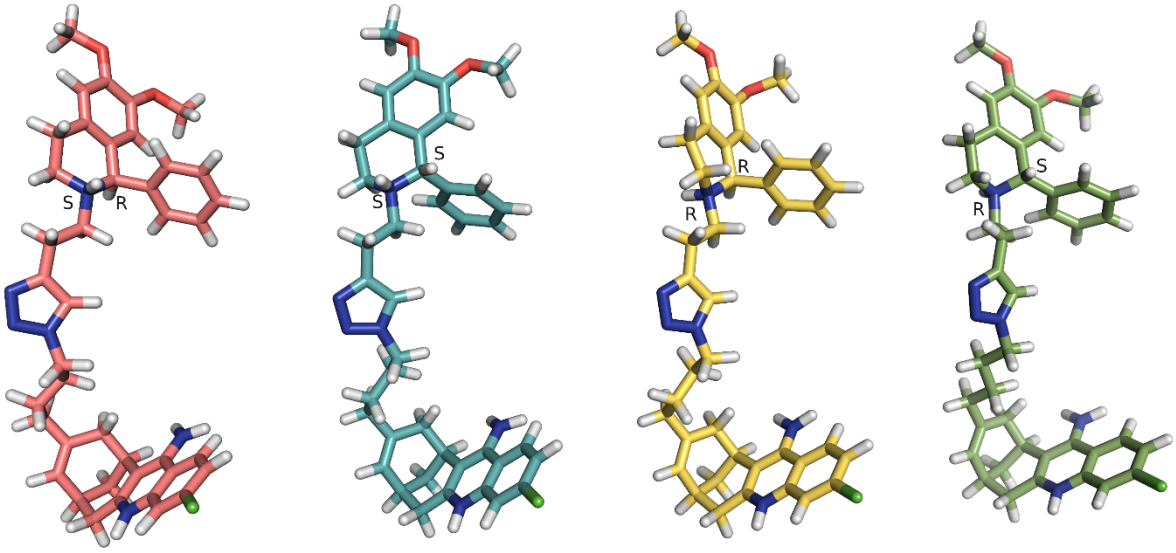

SR	**SS**		**RR**		**RS**			
	***Anti* isomer**							
Trp286 conformation	**Native**				**Sandwiched**			
Conformers	SR	SS	RR	RS	SR	SS	RR	RS
vina scoring kcal/mol after position restraint	-16.11	-16.00	-15.08	-16.16	-15.82	-14.05	-16.69	-17.00
vina scoring kcal/mol after 1 ns MD	**-16.08**	-15.71	-14.77	-15.44	-14.89	-15.62	-15.76	-14.72
	***Syn* isomer**							
Trp286 conformation	**Native**				**Sandwiched**			
Conformers	SR	SS	RR	RS	SR	SS	RR	RS
vina scoring kcal/mol after position restraint	-15.34	-14.65	-15.12	-15.34	-15.77	-16.19	-15.14	-16.53
vina scoring kcal/mol after 1 ns MD	-15.75	-14.66	**-16.35**	-14.03	-15.84	-16.04	-14.89	-15.68

III.2. Quantum Mechanical and Molecular Dynamics

All QM/MM calculations were carried out using the Gaussian 09 program.[17] The combination of QM and MM levels was realized following the ONIOM approach with mechanical embedding.[18] The QM layer included the substrate (97 atoms) while the protein and all water molecules were placed into the MM layer. No link atom appears in this partition, as the substrate is not covalently bonded to the protein. We used the same MM force field as for MD simulations: Amber99SB[11] is completed with Generalized Amber Force Field (GAFF) parameters[12] for the substrate and TIP3P for water molecules.[19] The quantum mechanical part was described at B97D/6-31G(d) level.[20] The structures were prepared from a selected snapshot of a protein-substrate complex in a water box after MD equilibration procedure. All water molecules beyond 5 Å from protein and substrate as well as all counter-ions were removed. Resulting *syn*- and *anti*-complexes were brought to the same stoichiometry (16673 atoms, Fig. 4). All structures were fully relaxed at QM/MM level (with complete relaxation of the system). The nature of all stationary points was confirmed by the frequency calculation on the substrate in the fixed protein environment. Interaction energies

were calculated on fixed minima geometries of the complexes according to $E_{int} = E_{complex} - E_{protein} - E_{substrate}$.

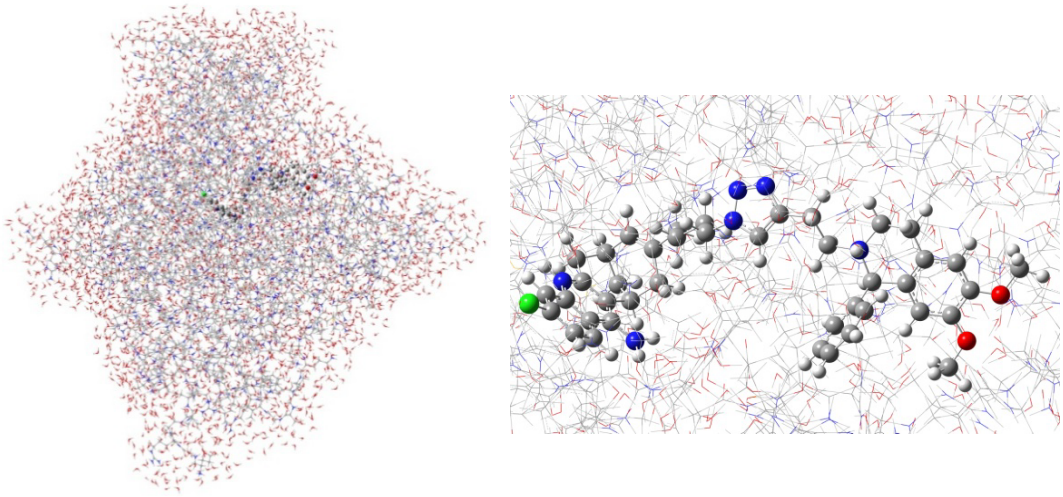

Figure 4. General view of AChE (left) and of substrate *anti*-9-HUPZ4PIQ-A2 inside (right).

IV. Copies of ^{1}H and ^{13}C NMR spectra

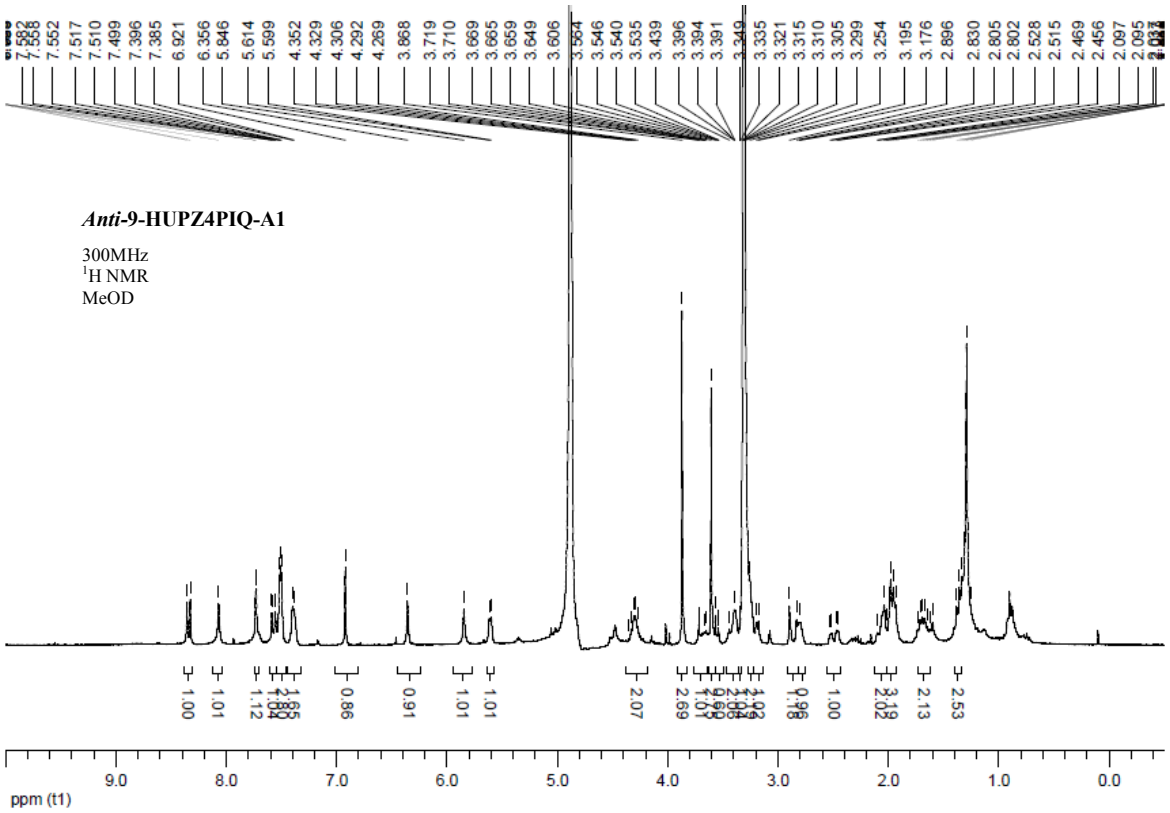

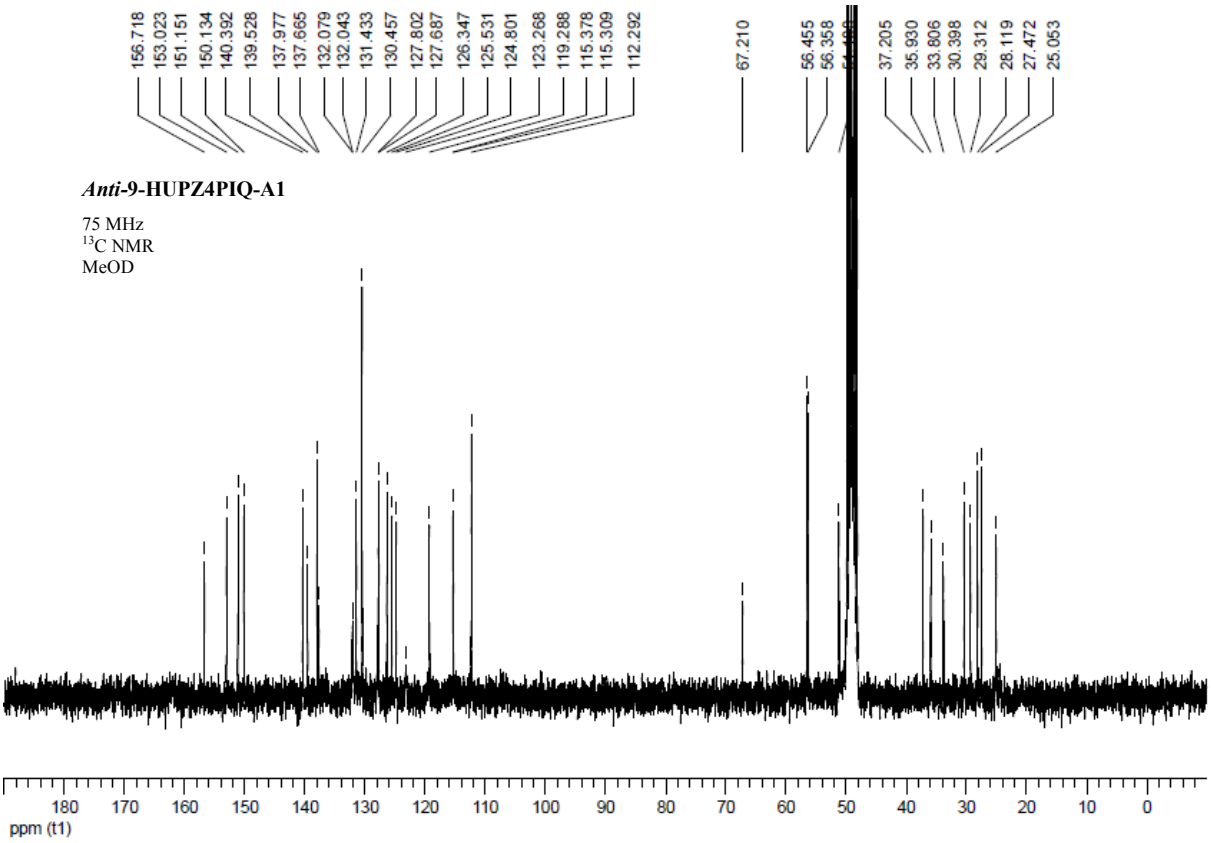

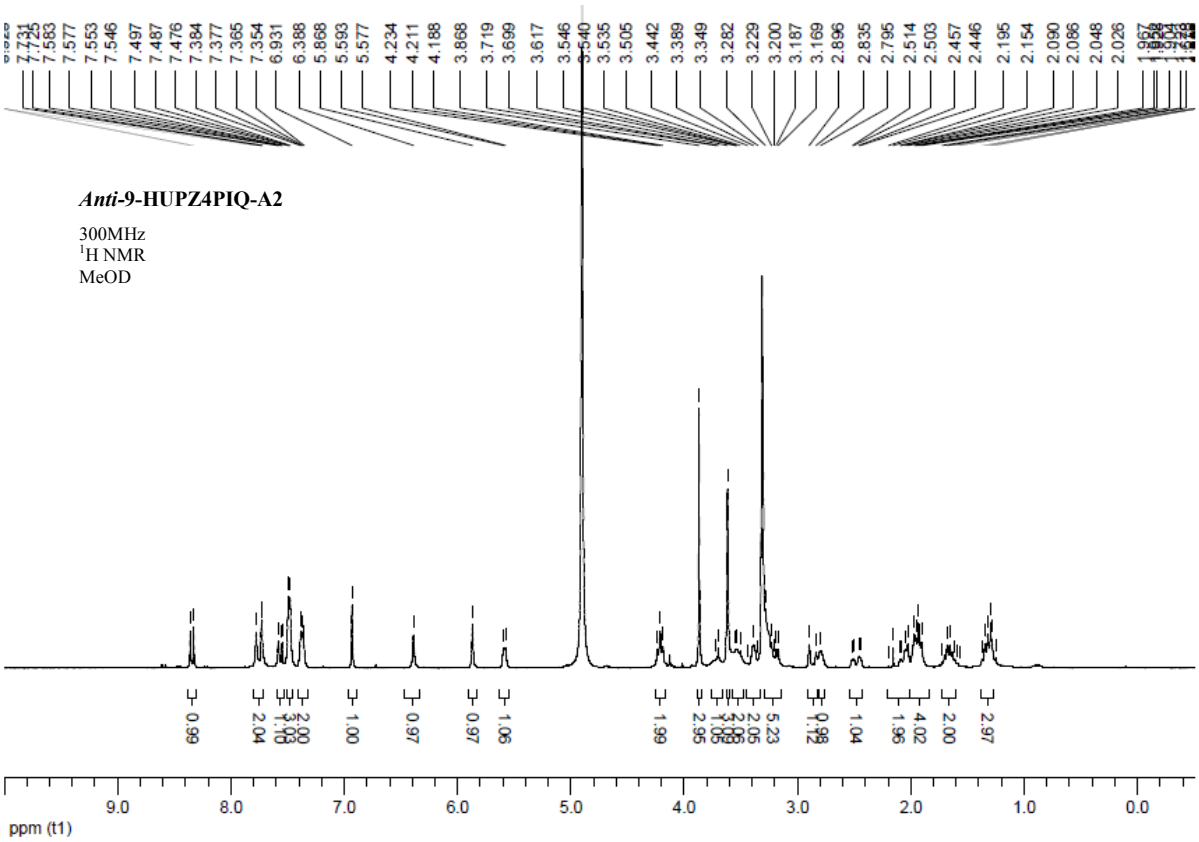
Anti-9-HUPZ4PIQ-A2
300MHz
1H NMR
MeOD
ppm (t1)

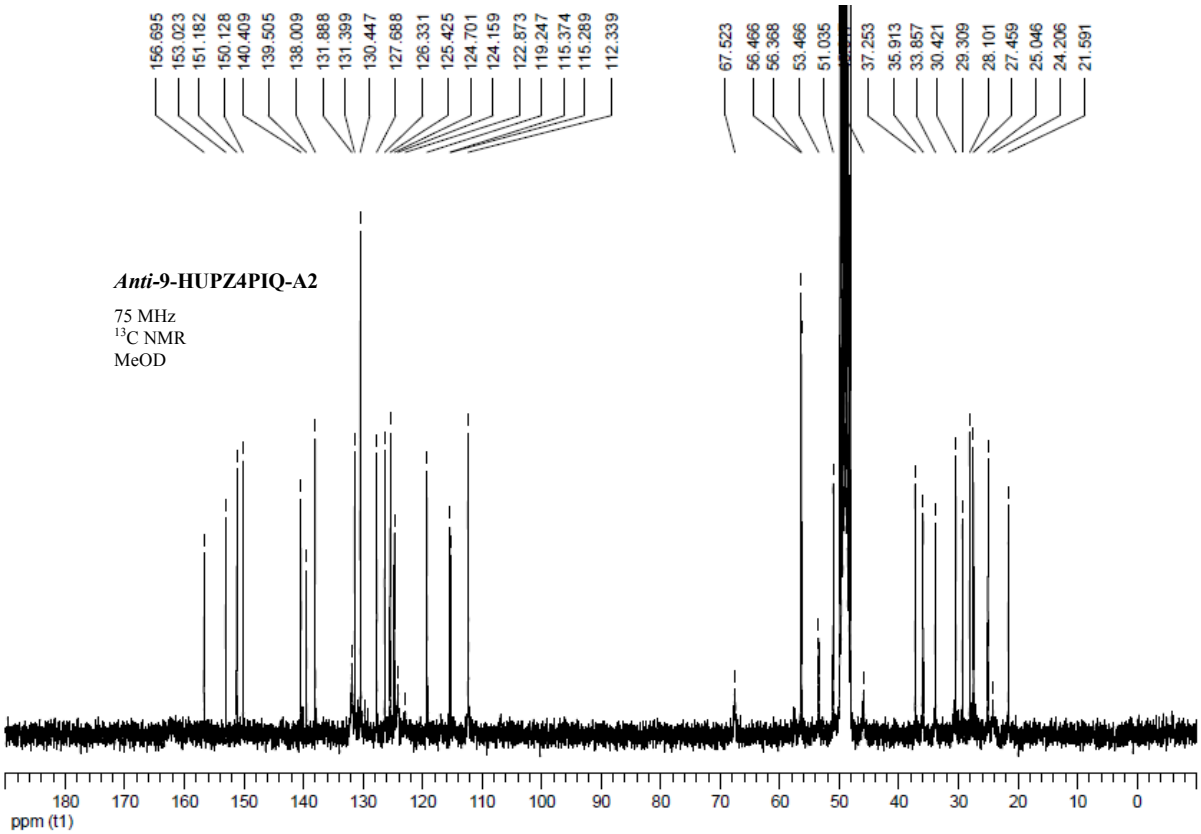
Anti-9-HUPZ4PIQ-A2
75 MHz
13C NMR
MeOD
ppm (t1)

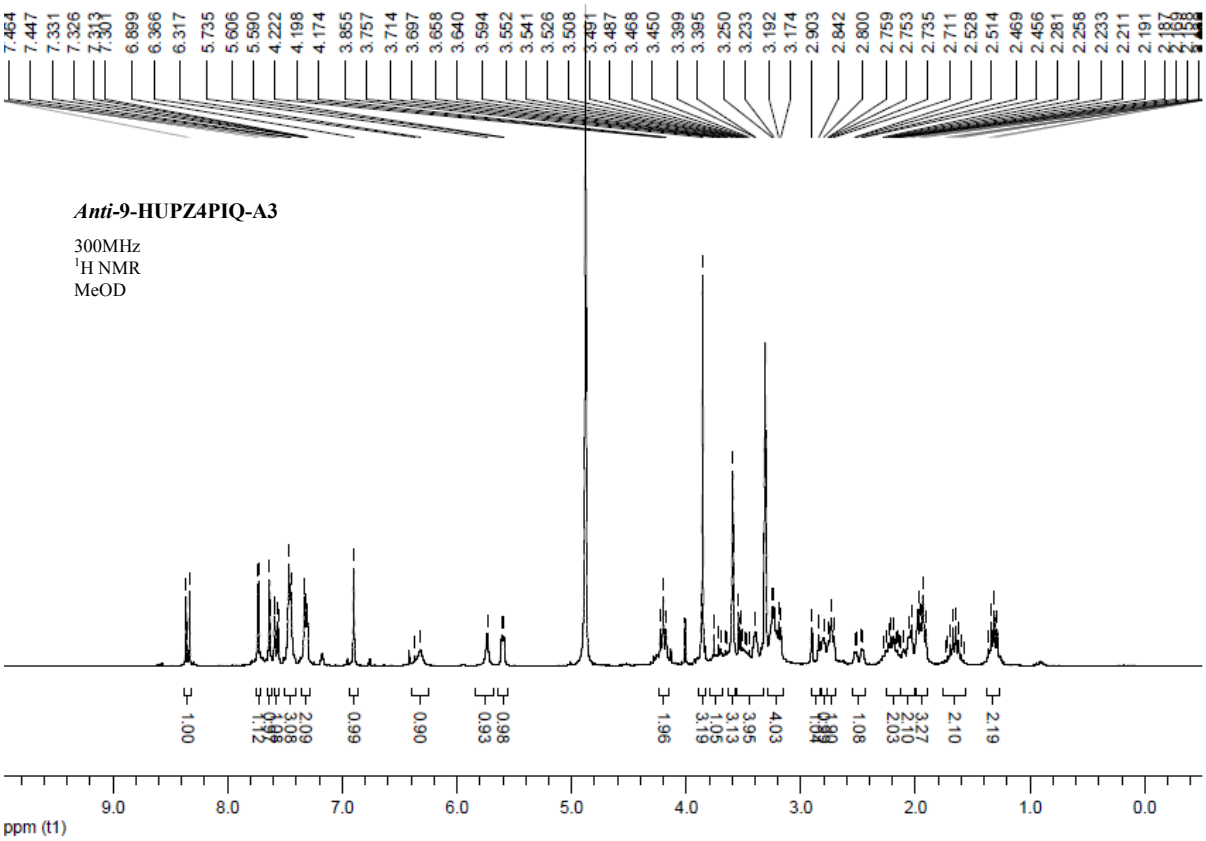
7.464
7.447
7.331
7.326
7.313
7.301
6.899
6.366
6.317
5.735
5.606
5.590
4.222
4.198
4.174
3.855
3.757
3.714
3.697
3.658
3.640
3.594
3.552
3.541
3.526
3.508
3.491
3.487
3.468
3.450
3.399
3.395
3.250
3.233
3.192
3.174
2.903
2.842
2.800
2.759
2.753
2.735
2.711
2.528
2.514
2.469
2.456
2.281
2.258
2.233
2.211
2.191
Anti-9-HUPZ4PIQ-A3
300MHz
1H NMR
MeOD
1.00
1.12
2.08
0.99
0.90
0.93
0.88
1.96
3.19
3.13
3.95
4.03
1.08
2.03
2.27
2.10
2.19
9.0
8.0
7.0
6.0
5.0
4.0
3.0
2.0
1.0
0.0
ppm (t1)

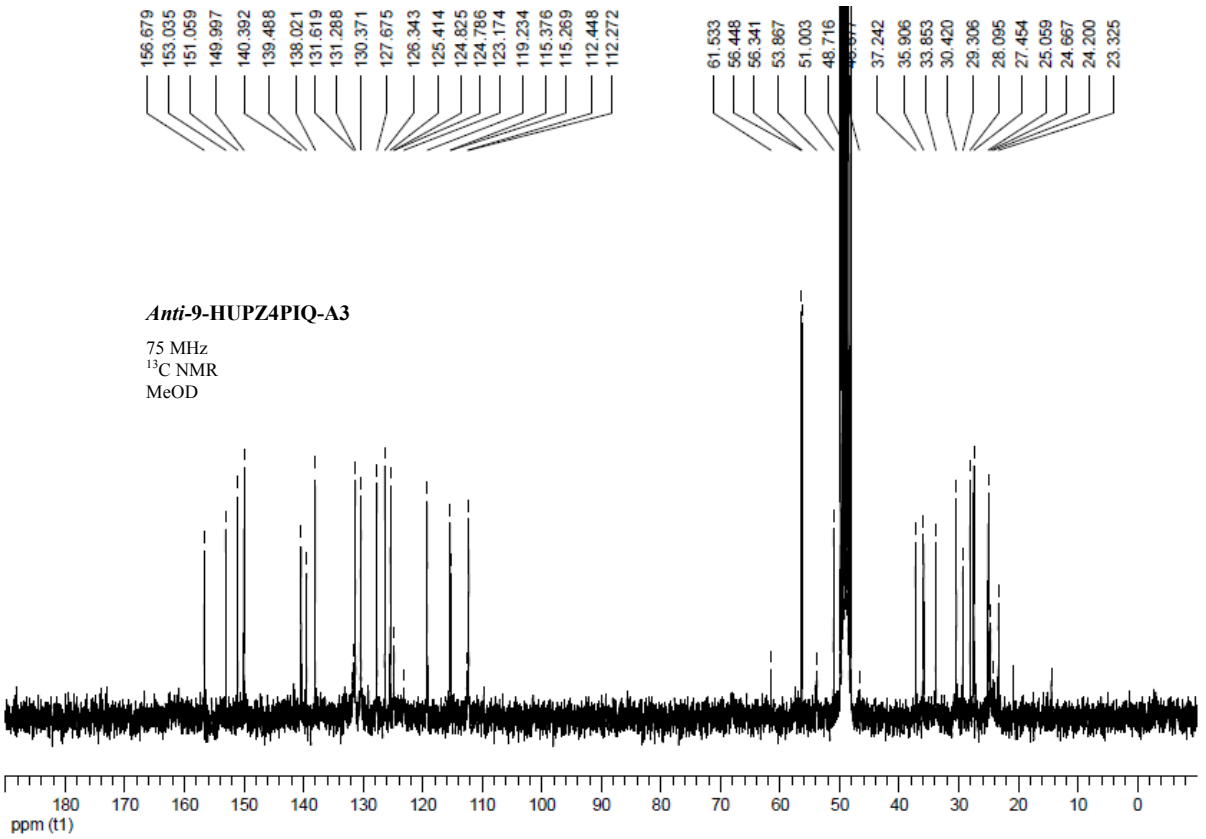
156.679
153.035
151.059
149.997
140.392
139.488
138.021
131.619
131.288
130.371
127.675
126.343
125.414
124.825
124.786
123.174
119.234
115.376
115.269
112.448
112.272
61.533
56.448
56.341
53.867
51.003
48.716
37.242
35.906
33.853
30.420
29.306
28.095
27.454
25.059
24.667
24.200
23.325
Anti-9-HUPZ4PIQ-A3
75 MHz
13C NMR
MeOD
180
170
160
150
140
130
120
110
100
90
80
70
60
50
40
30
20
10
0
ppm (t1)

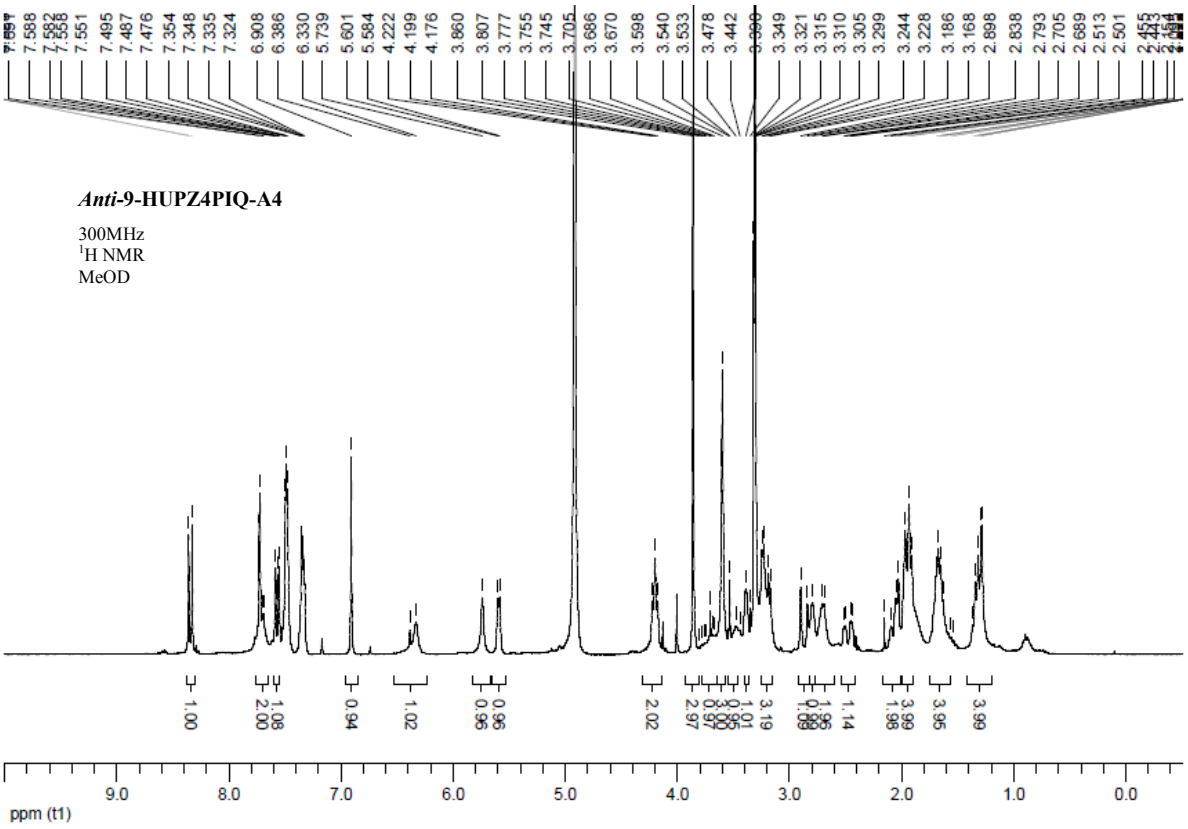

***Anti*-9-HUPZ4PIQ-A4**

300MHz
^{1}H NMR
MeOD

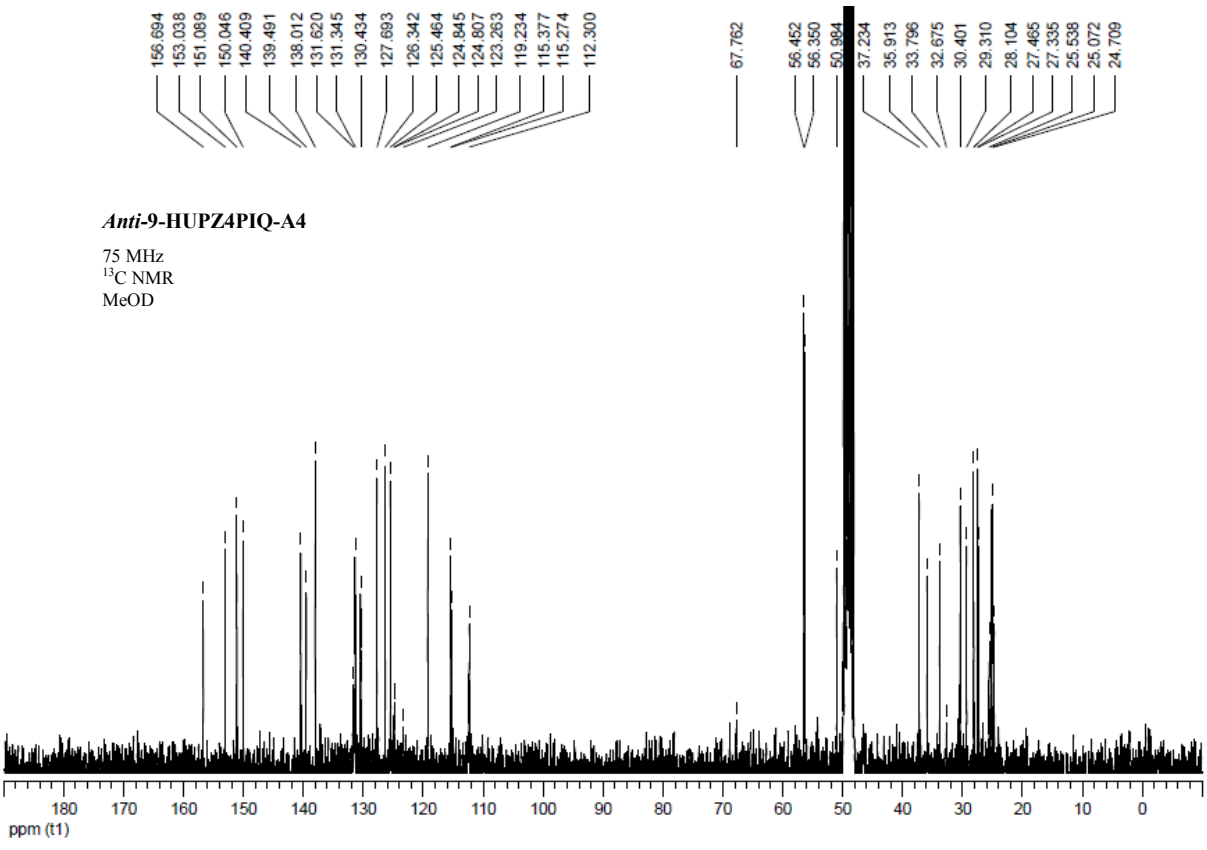

***Anti*-9-HUPZ4PIQ-A4**

75 MHz
^{13}C NMR
MeOD

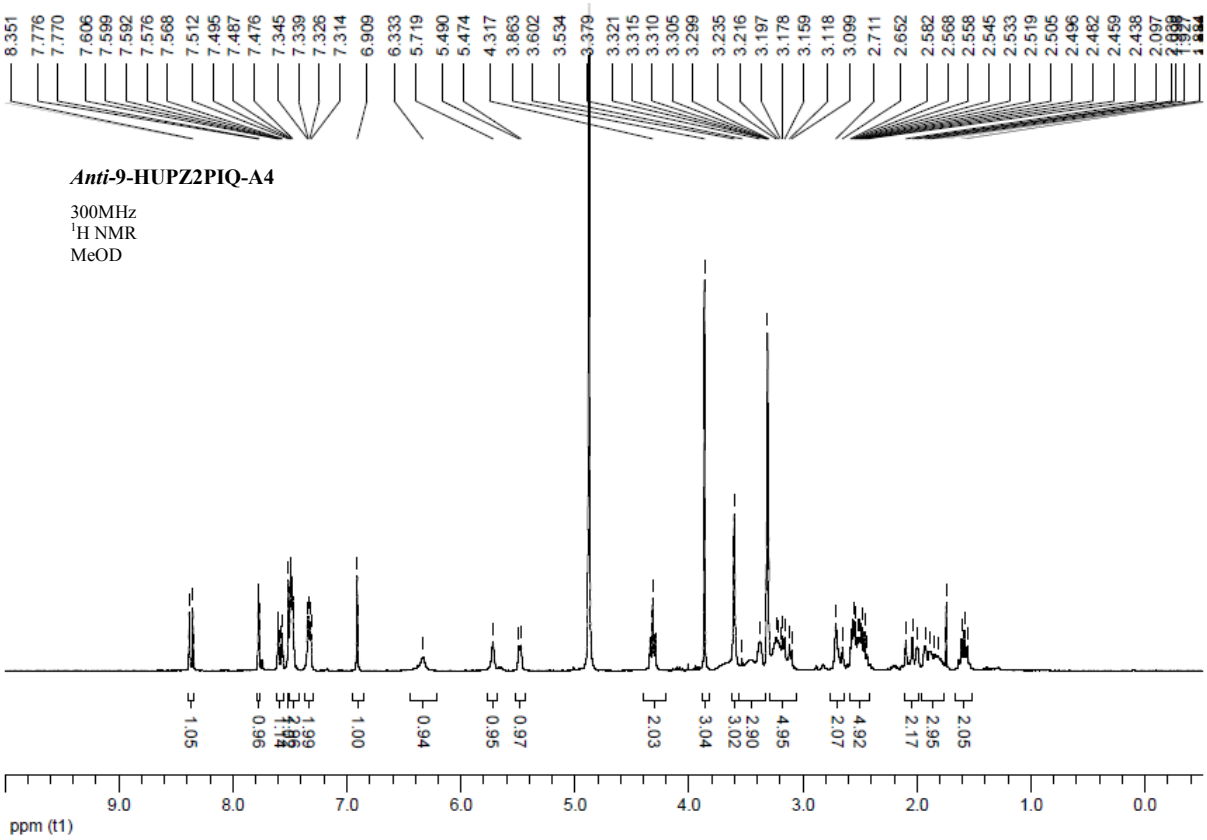

***Anti*-9-HUPZ2PIQ-A4**

300MHz
^{1}H NMR
MeOD

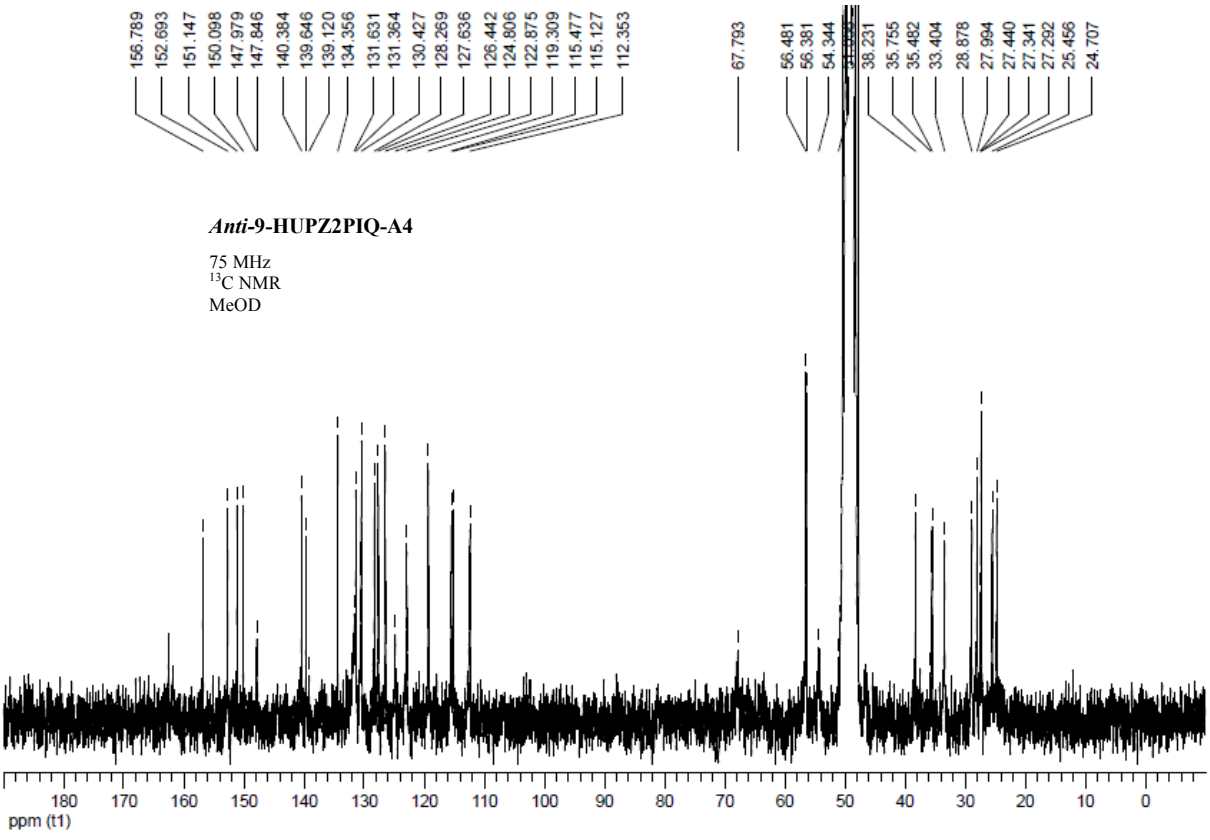

***Anti*-9-HUPZ2PIQ-A4**

75 MHz
^{13}C NMR
MeOD

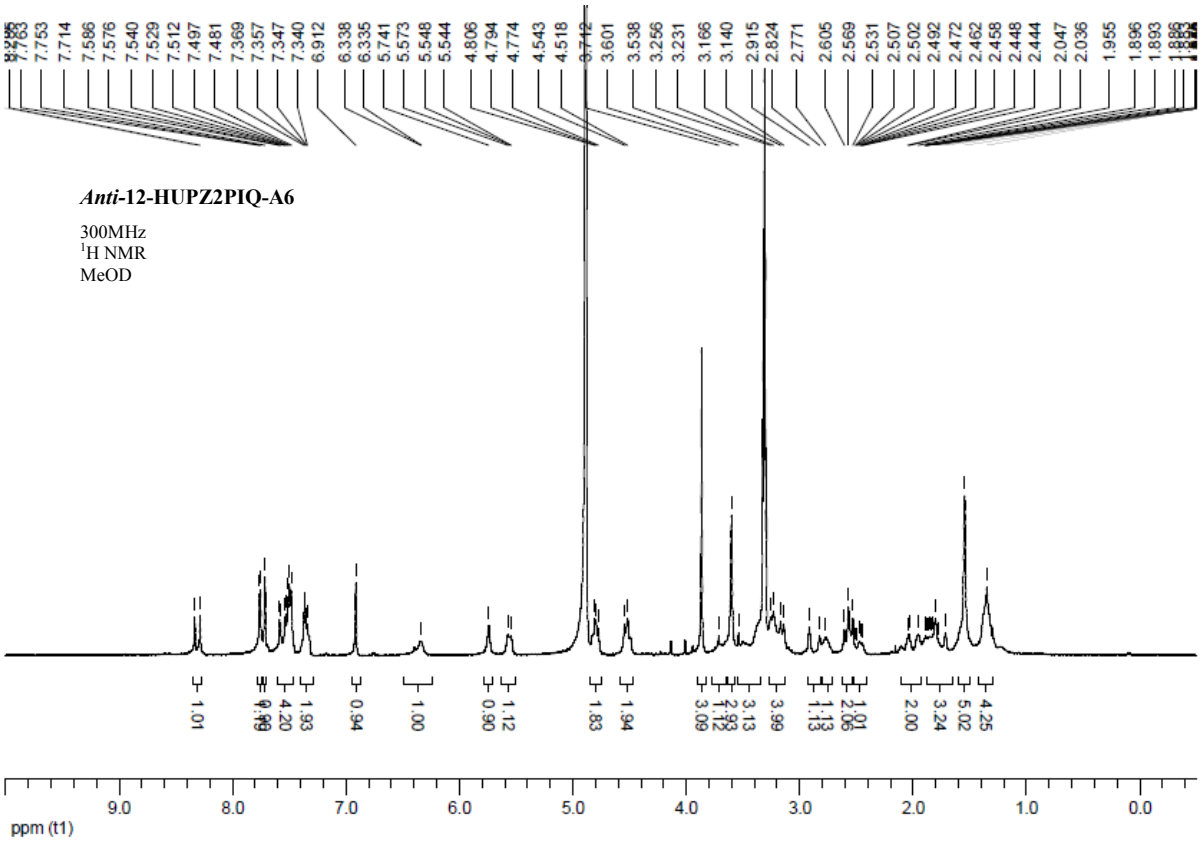

***Anti*-12-HUPZ2PIQ-A6**

300MHz
^{1}H NMR
MeOD

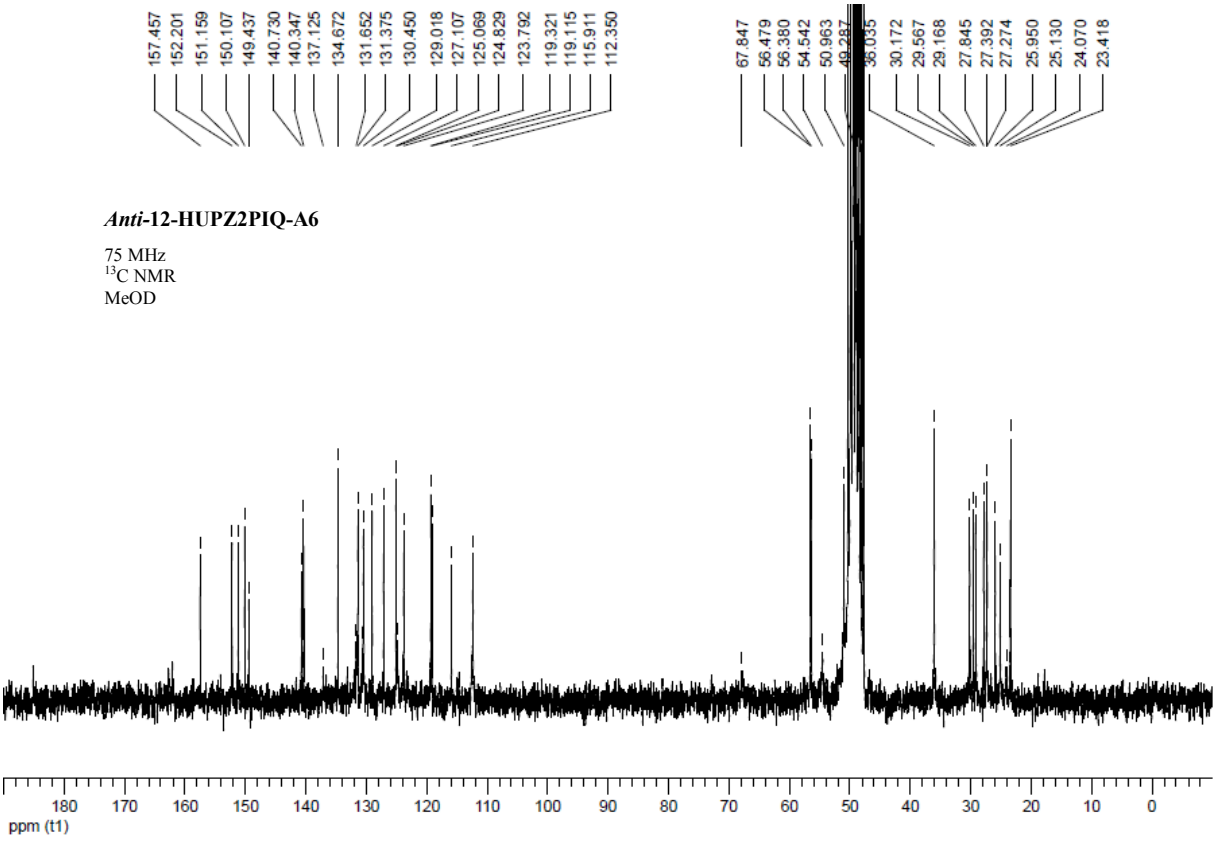

***Anti*-12-HUPZ2PIQ-A6**

75 MHz
^{13}C NMR
MeOD

V. RP-HPLC elution profile (system C)

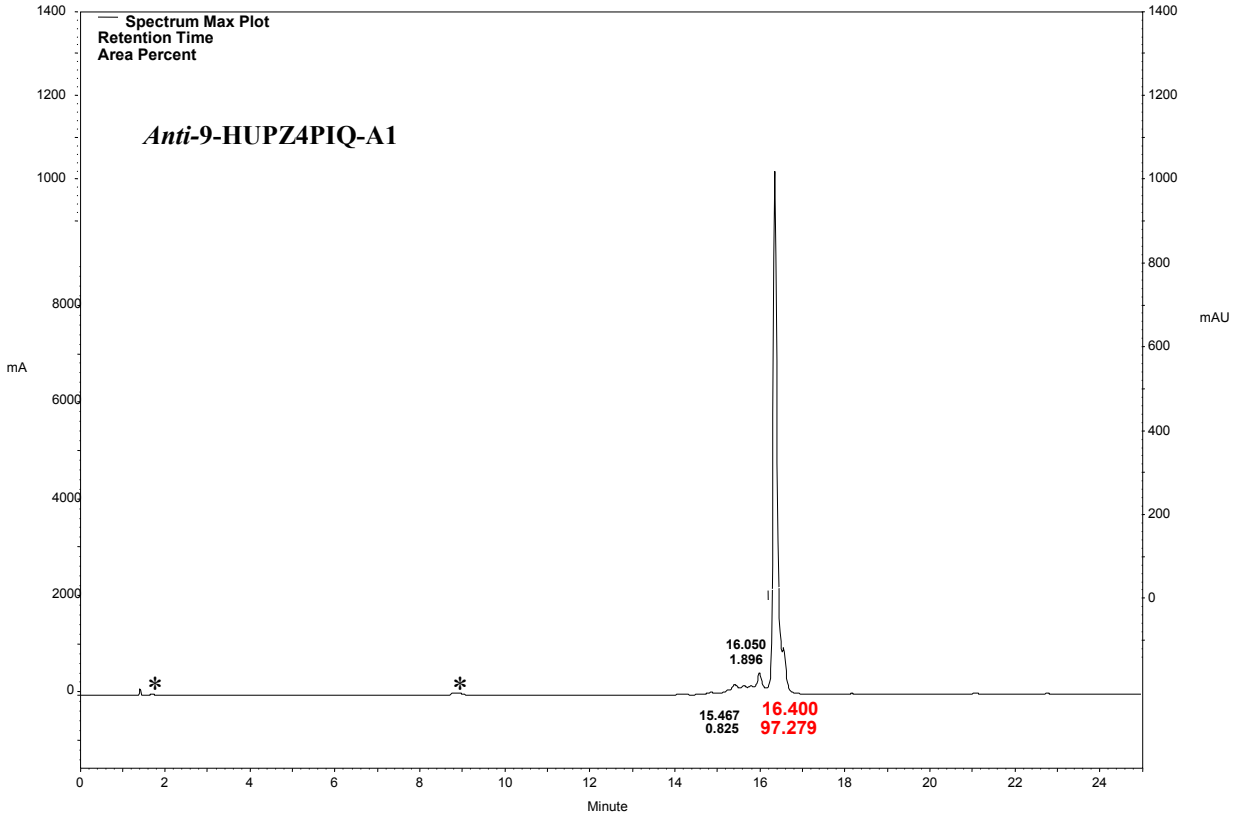

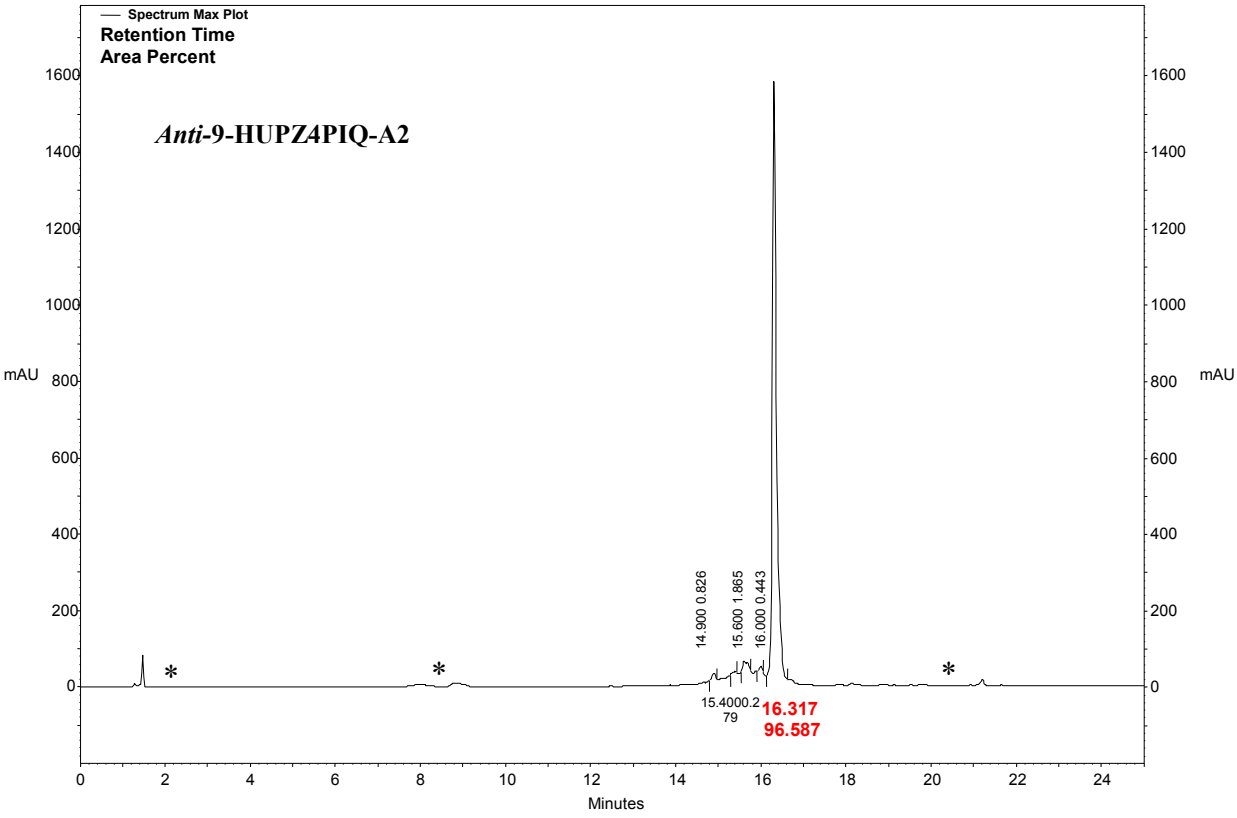

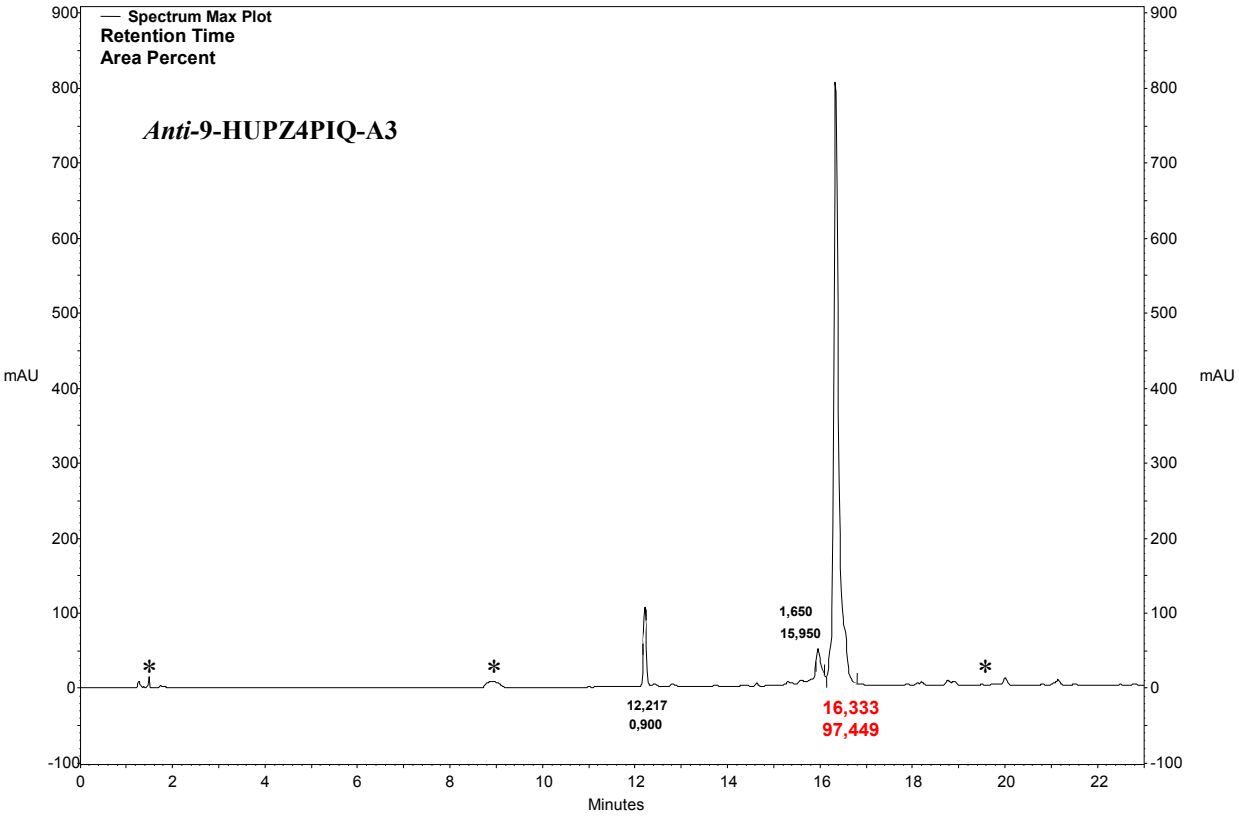
Spectrum Max Plot
Retention Time
Area Percent
Anti-9-HUPZ4PIQ-A3
mAU
Minutes
1,650
15,950
12,217
0,900
16,333
97,449

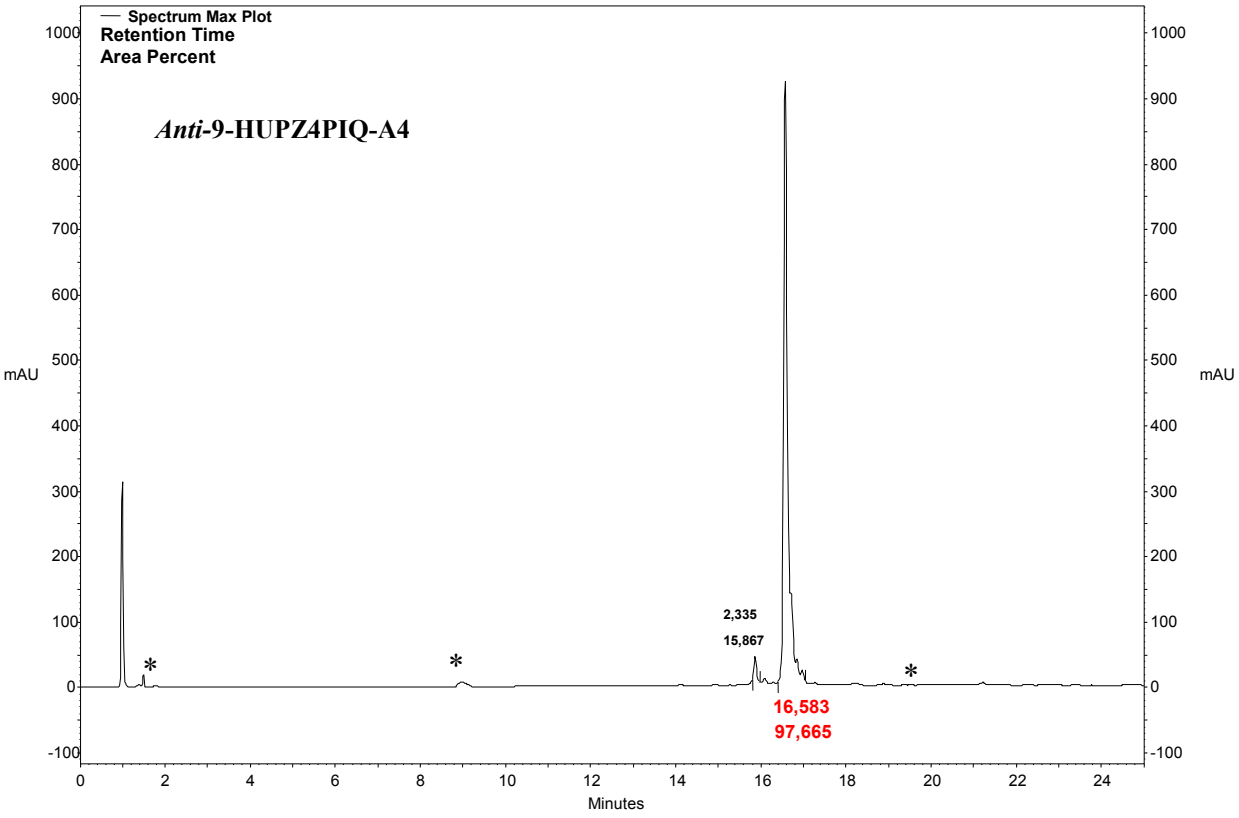
Spectrum Max Plot
Retention Time
Area Percent
Anti-9-HUPZ4PIQ-A4
mAU
Minutes
2,335
15,867
16,583
97,665

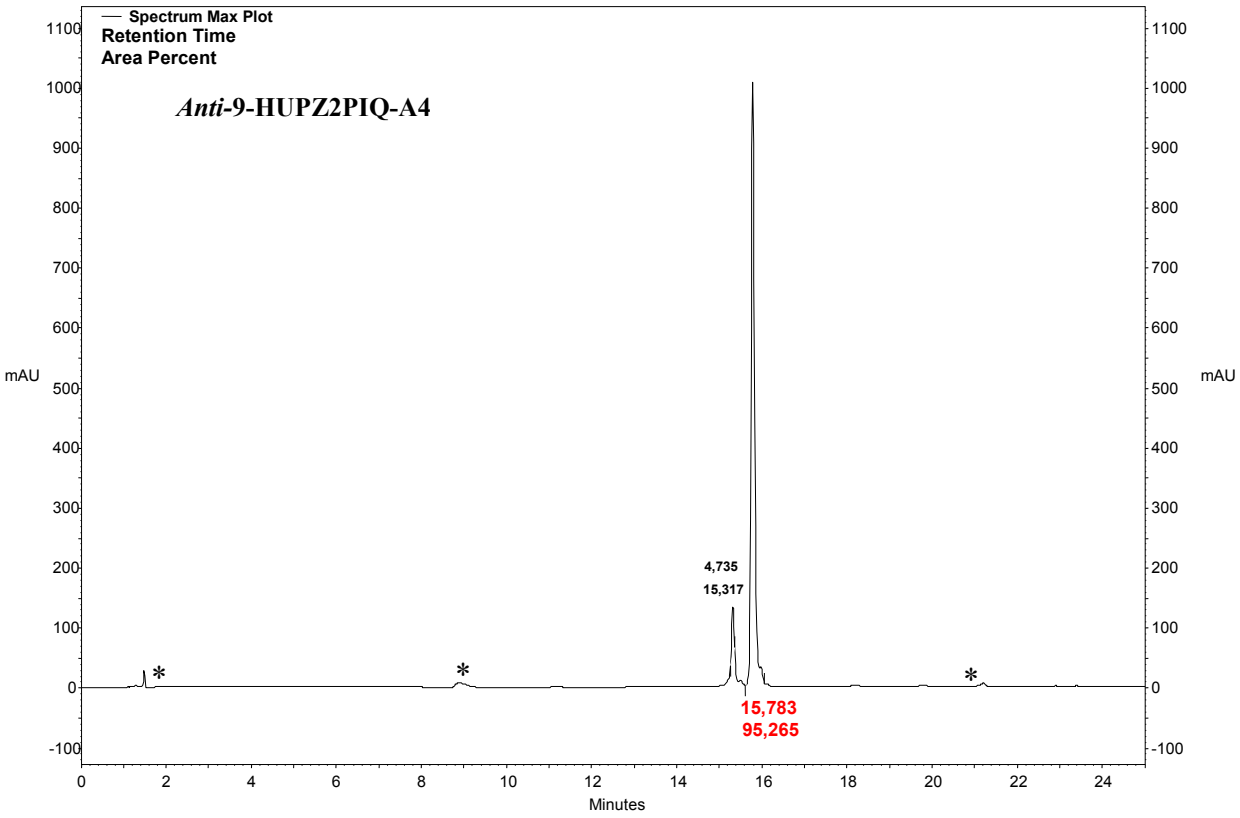

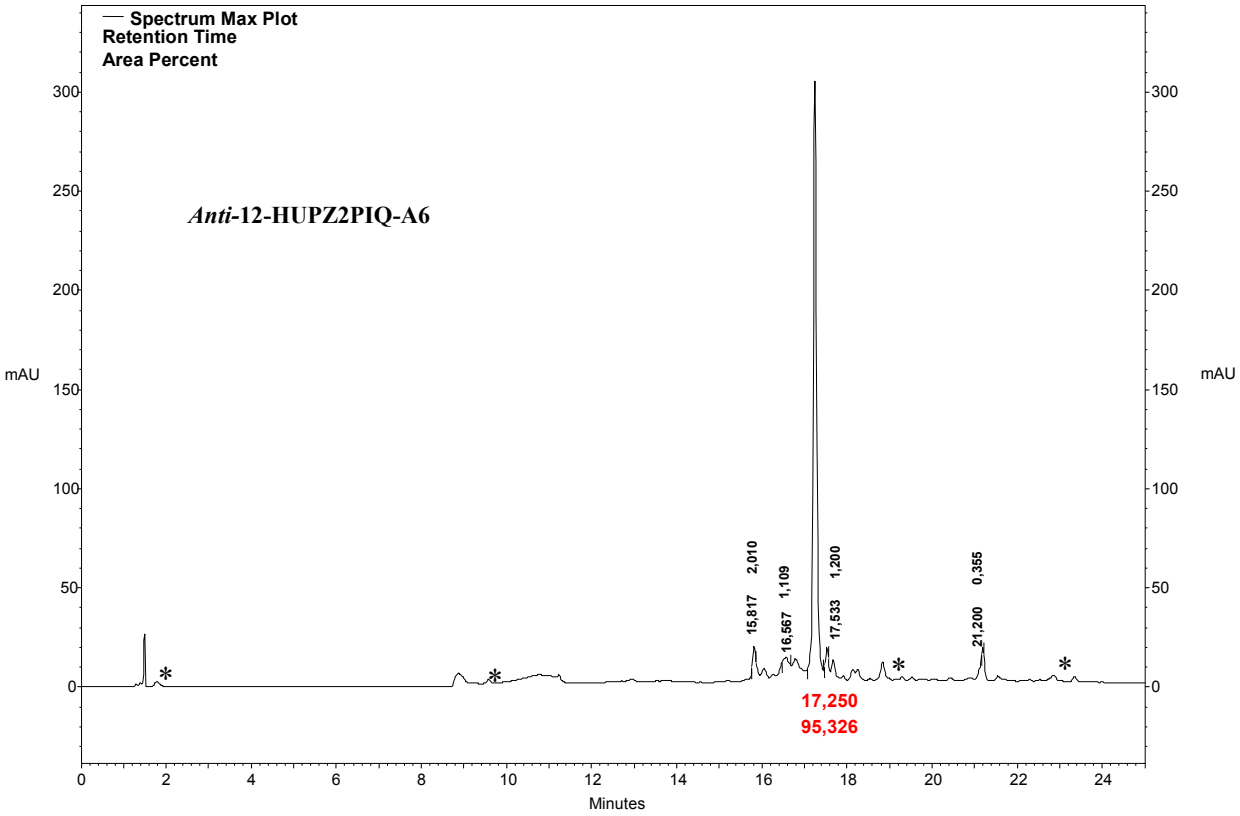

* Peaks found in the aq HPLC mobile phase

VI. References

1. G. R. Fulmer, A. J. M. Miller, N. H. Sherden, H. E. Gottlieb, A. Nudelman, B. M. Stoltz, J. E. Bercaw and K. I. Goldberg, *Organometallics*, 2010, **29**, 2176-2179.
2. C. Ronco, G. Sorin, F. Nachon, R. Foucault, L. Jean, A. Romieu and P.-Y. Renard, *Bioorg. Med. Chem.*, 2009, **17**, 4523-4536.
3. C. Ronco, R. Foucault, E. Gillon, P. Bohn, F. Nachon, L. Jean and P.-Y. Renard, *ChemMedChem*, 2011, **6**, 876-888.
4. C. Ronco, E. Carletti, J.-P. Colletier, M. Weik, F. Nachon, L. Jean and P.-Y. Renard, *ChemMedChem*, 2012, **7**, 400-405.
5. G. Mercey, J. Renou, T. Verdelet, M. Kliachyna, R. Baati, E. Gillon, M. Arboléas, M. Loiodice, F. Nachon, L. Jean and P.-Y. Renard, *J. Med. Chem.*, 2012, **55**, 10791-10795.
6. G. Mercey, T. Verdelet, G. Saint-Andre, E. Gillon, A. Wagner, R. Baati, L. Jean, F. Nachon and P.-Y. Renard, *Chem. Commun.*, 2011, **47**, 5295-5297.
7. A. Krasiński, Z. Radić, R. Manetsch, J. Raushel, P. Taylor, K. B. Sharpless and H. C. Kolb, *J. Am. Chem. Soc.*, 2005, **127**, 6686-6692.
8. F. Nachon, Y. Nicolet, N. Viguié, P. Masson, J. Fontecilla-Camps and O. Lockridge, *Eur. J. Biochem.*, 2002, **269**, 630-637.
9. E. Carletti, J.-P. Colletier, M. T. F. Dupeux, P. Masson and F. Nachon, *J. Med. Chem.*, 2010, **53**, 4002-4008.
10. G. L. Ellman, K. D. Courtney, B. J. Andres and R. M. Featherstone, *Biochem. Pharmacol.*, 1961, **7**, 88-95.
11. E. Carletti, H. Li, B. Li, F. Ekström, Y. Nicolet, M. Loiodice, E. Gillon, M. T. Froment, O. Lockridge, L. M. Schopfer, P. Masson and F. Nachon, *J. Am. Chem. Soc.*, 2008, **130**, 16011-16020.
12. F. Nachon, E. Carletti, C. Ronco, M. Trovaslet, Y. Nicolet, L. Jean and P.-Y. Renard, *Biochem. J.*, 2013.
13. N. Eswar, B. Webb, M. A. Marti-Renom, M. Madhusudhan, D. Eramian, M.-Y. Shen, U. Pieper and A. Sali, *Curr. Protoc. Protein Sci.*, John Wiley & Sons, Inc., 2001.
14. P. D. Adams, P. V. Afonine, G. Bunkoczi, V. B. Chen, I. W. Davis, N. Echols, J. J. Headd, L. W. Hung, G. J. Kapral, R. W. Grosse-Kunstleve, A. J. McCoy, N. W. Moriarty, R. Oeffner, R. J. Read, D. C. Richardson, J. S. Richardson, T. C. Terwilliger and P. H. Zwart, *Acta Crystallogr. D Biol. Crystallogr.*, 2010, **66**, 213-221.
15. B. Hess, C. Kutzner, D. van der Spoel and E. J. Lindahl, *Chem. Theory Comput.*, 2008, **4**, 435-447.
16. V. Hornak, R. Abel, A. Okur, B. Strockbine, A. Roitberg and C. Simmerling, *Proteins Struct. Funct. Bioinf*, 2006, **65**, 712-725.
17. J. Wang, R. M. Wolf, J. W. Caldwell, P. A. Kollman and D. A. Case, *J. Comput. Chem.*, 2004, **25**, 1157-1174.
18. H. J. C. Berendsen, J. P. M. Postma, W. F. van Gunsteren, A. DiNola and J. R. Haak, *J. Chem. Phys.*, 1984, **81**, 3684-3690.
19. B. Hess, H. Bekker, H. J. C. Berendsen and J. G. E. M. Fraaije, *J. Comput. Chem.*, 1997, **18**, 1463-1472.
20. O. Trott and A. J. Olson, *J. Comput. Chem.*, 2010, **31**, 455-461.
21. G. M. Morris, R. Huey, W. Lindstrom, M. F. Sanner, R. K. Belew, D. S. Goodsell and A. J. Olson, *J. Comput. Chem.*, 2009, **16**, 2785-2791.
22. R. Gaussian 09, M. J. Frisch, G. W. Trucks, H. B. Schlegel, G. E. Scuseria, M. A. Robb, J. R. Cheeseman, G. Scalmani, V. Barone, B. Mennucci, G. A. Petersson, H. Nakatsuji, M. Caricato, X. Li, H. P. Hratchian, A. F. Izmaylov, J. Bloino, G. Zheng, J. L. Sonnenberg,

M. Hada, M. Ehara, K. Toyota, R. Fukuda, J. Hasegawa, M. Ishida, T. Nakajima, Y. Honda, O. Kitao, H. Nakai, T. Vreven, J. J. A. Montgomery, J. E. Peralta, F. Ogliaro, M. Bearpark, J. J. Heyd, E. Brothers, K. N. Kudin, V. N. Staroverov, R. Kobayashi, J. Normand, K. Raghavachari, A. Rendell, J. C. Burant, S. S. Iyengar, J. Tomasi, M. Cossi, N. Rega, J. M. Millam, M. Klene, J. E. Knox, J. B. Cross, V. Bakken, C. Adamo, J. Jaramillo, R. Gomperts, R. E. Stratmann, O. Yazyev, A. J. Austin, R. Cammi, C. Pomelli, J. W. Ochterski, R. L. Martin, K. Morokuma, V. G. Zakrzewski, G. A. Voth, P. Salvador, J. J. Dannenberg, S. Dapprich, A. D. Daniels, Ö. Farkas, J. B. Foresman, J. V. Ortiz, J. Cioslowski and D. J. Fox, Gaussian, Inc., WallingfordCT, 2009.

23. T. Vreven, K. S. Byun, I. Komáromi, S. Dapprich, J. J. A. Montgomery, K. Morokuma and M. J. Frisch, *J. Chem. Theory Comput.*, 2006, **2**, 815-826.
24. W. L. Jorgensen, J. Chandrasekhar, J. D. Madura, R. W. Impey and M. L. Klein, *J. Chem. Phys.*, 1983, **79**, 926-935.
25. S. Grimme, *J. Comp. Chem.*, 2006, **27**, 1787-1799.